Kinetics of Morphological Transitions in Microphase-Separated Diblock Copolymers

Kohtaro Yamada,† Makiko Nonomura,† and Takao Ohta*,‡

Department of Mathematical and Life Sciences, Graduate School of Science, Hiroshima University, Higashi-Hiroshima 739-8526, Japan, and Yukawa Institute for Theoretical Physics, Kyoto University, Kyoto 606-8502, Japan

Received February 15, 2004; Revised Manuscript Received May 17, 2004

ABSTRACT: We study morphological transitions between microphase-separated structures in diblock copolymers. By means of the two-mode approximation, kinetics of order−disorder (ODT) and order−order transitions (OOT) in the weak-segregation limit are investigated by solving numerically a coupled set of the amplitude equations for the fundamental modes. Breakup and reconnection of domains during the morphological transitions are explored in detail. Furthermore, we identify the metastable or unstable intermediate structures which appear in the process of ODT and OOT. The linear stability analysis is also applied to see the most unstable mode when a lamellar structure is destabilized.

1. Introduction

Diblock copolymers have been studied for many years with tremendous scientific interest due to their ability to self-assemble into various ordered microstructures.[1] The equilibrium morphological behaviors are now well understood, which depend on the block ratio and temperature as a consequence of segregation between different types of block chain comprising the polymer molecules. Besides three conventional microphase structures, i.e., lamellae (LAM), hexagonally packed cylinders (HEX), and spheres in body-centered-cubic (BCC) lattices, complex structures have also been observed such as gyroid structure (G). Gyroid is a bicontinuous cubic structure with $Ia\bar{3}d$ symmetry, in which the minority domain forms interweaving left- and right-handed 3-fold coordinated lattices. Typically, gyroid phase exists in a narrow region between lamellar and cylinder phase.[2,3] See ref 4 for a review of equilibrium phase behavior.

In the past decade, there are several experimental studies relevant to order−order transitions (OOT) and order−disorder transitions (ODT) in various block copolymers.[5−30] These experiments have been carried out by using scattering techniques, transmission electron microscopy, and rheological measurements. Diblock copolymer solutions and melts exhibit the following OOTs by changing temperature: BCC ↔ HEX,[13−15] LAM ↔ HEX,[16] HEX ↔ G,[17−19] LAM ↔ G.[20−24] Furthermore, the transition between face-centered-cubic and BCC structures, which is driven by decreasing solvent selectivity with increasing temperature, has been studied in diblock copolymer solution.[25]

Quite recently, kinetics of morphological transitions have been investigated experimentally. It has been found that the transitions often involve intermediate structures such as hexagonally perforated layers phase (HPL) for both the LAM → G and BCC → G.[17,24] In addition, experiments of OOTs are conducted not only for diblock copolymers but also for other systems. For example, experimental measurements in triblock copolymers for LAM ↔ HEX[26,27] and HEX ↔ BCC[28−30] transitions have been reported. The kinetics of transitions and dynamics of concentration fluctuations have also been investigated in surfactant systems, where mesoscopic domain structures similar to those of block copolymers are formed.[31−36]

On the theoretical side, there are a number of studies of the equilibrium properties.[1−3] The self-consistent-field theory has been applied to investigate the kinetic pathways of HEX ↔ BCC, HEX → LAM, G ↔ HEX, evaluating the free energy landscape.[37−39] (The conclusion about gyroid in ref 37 is inconsistent with other theories and experiments. See ref 40.) However, theoretical investigation of the kinetics and the mechanism of the transitions have received relatively little attention with a few exceptions. In the case of the LAM ↔ HEX transition, the front propagation velocity for stable phases invading metastable phases is evaluated.[41] For weakly segregated diblock copolymer systems, numerical simulations based on the single-mode expansion have been performed by a time-dependent Ginzburg−Landau approach[42−45] for LAM, HEX, and BCC structures. However, the gyroid morphology cannot be represented by the single mode expansion.

The purpose of the present paper is to study the dynamics of structural transitions in diblock copolymer melts extending our previous theory[45] to the two-mode expansion. We focus our attention on the transitions which involve the gyroid structures. Starting with the time evolution equation for the local volume fraction of monomers,[46] we derive a coupled set of equations for the amplitude of each fundamental mode. It is noted that the mode expansion is justified in the weak segregation regime and that this is the very condition that the G structure appears. Therefore, we emphasize that the present theory has a complete internal consistency. Our preliminary results have been published in ref 47.

The present theory has several limitations. Most crucial is that the amplitudes of the fundamental modes are assumed to be space independent. Therefore, coexistence of two different structures and nucleation of a new structure in the matrix of a metastable phase are not described.

† Hiroshima University.
‡ Kyoto University.
* To whom correspondence should be addressed. E-mail: takao@yukawa.kyoto-u.ac.jp.

10.1021/ma049687o CCC: $27.50
Published on Web 07/01/2004

Nevertheless, the mode expansion method is useful to clarify the basic properties of the morphological transitions. First of all, the amplitude equations exhibit many equilibrium solutions apart from the most stable LAM, HEX, G, and BCC. This fact enables us to examine the candidate of the metastable structures which appear in the course of the transitions. In fact, by solving the amplitude equations starting from one structure to another more stable structure, we can investigate formation of possible intermediate structures and identify it without ambiguity. For example, we shall show that an *Fddd* structure exists as a metastable structure and HPL also appears during the transition, but the latter is not an equilibrium structure but a transient one.

The organization of the paper is as follows. In section 2, we introduce the free energy functional and the kinetic equation for diblock copolymers. In section 3, we describe the two-mode expansion and derive a coupled set of equations for the amplitude of each fundamental mode. This method is justified in the weak segregation limit. The equilibrium phase diagram obtained by solving the amplitude equations are presented in section 4. We argue some metastable phases which are the stable equilibrium solutions but have larger free energies. The kinetics of ODT and OOT are explored numerically in sections 5 and 6, respectively. In section 7, we show the results of a linear stability analysis for a lamellar structure. Summary and discussion are given in section 8. In Appendix A, all the amplitude equations are listed explicitly whereas the form of the free energy in terms of the amplitudes are given in Appendix B. The metastable solutions of the amplitude equations which are not described in the text are presented in Appendix C.

2. Kinetic Equations

The kinetic equation for A−B type diblock copolymers is given by the following time evolution equation:[46]

$$\frac{\partial \phi}{\partial t} = \nabla^2 \frac{\delta F}{\delta \phi} \tag{1}$$

where $\phi = \phi_A - \phi_B$, where ϕ_A (ϕ_B) is the local volume fraction of the A (B) monomers. The incompressibility condition $\phi_A + \phi_B = 1$ has been assumed. The free energy functional F is given by[48]

$$F\{\phi\} = \int d\vec{r} \left[\frac{1}{2}(\nabla\phi)^2 + W(\phi)\right] + \frac{\alpha}{2}\int d\vec{r} \int d\vec{r}\,' G(\vec{r}, \vec{r}\,')(\phi(\vec{r}) - \bar{\phi})(\phi(\vec{r}\,') - \bar{\phi}) \tag{2}$$

where the parameter α is positive and $\bar{\phi}$ is the spatial average of ϕ. The second term represents a long-range interaction which originates from the connectedness of A and B blocks at a junction point in each polymer chain. The function $G(\vec{r}, \vec{r}\,')$ is defined through the relation

$$-\nabla^2 G = \delta(\vec{r} - \vec{r}\,') \tag{3}$$

The function $W(\phi)$ is given in weak segregation by

$$W(\phi) = -\frac{\tau}{2}\phi^2 + \frac{g}{4}\phi^4 \tag{4}$$

where the coefficient g is assumed to be positive. The parameter τ is negative for the high-temperature uniform phase, whereas it is positive for the microphase-separated state at low temperature.

Substituting eq 2 into eq 1, the time evolution equation is written as

$$\frac{\partial \phi}{\partial t} = \nabla^2(-\nabla^2\phi - \tau\phi + g\phi^3) - \alpha(\phi - \bar{\phi}) \tag{5}$$

This equation (or the free energy (2)) is probably the simplest one which contains the essential property of diblock copolymer melts. As mentioned above, the long-range interaction in eq 5 is the consequence of the osmotic incompressibility independent of the approximations used and the microscopic details of the system. Therefore, eq 2 enables us to study the universal features of microphase separation. So far the free energy (2) (and hence eq 5) has been restricted to AB diblock copolymers. However, there is an attempt to generalize the free energy to block copolymers having any topological structure including ABA triblocks.[49]

Equation 5 has been used for numerical simulations to study the kinetics of microphase separation not only in two dimensions but also in three dimensions.[45] However, a gyroid structure has not been examined. Quite recently, Teramoto and Nishiura[50] have shown, by using three-dimensional simulations, that eq 5 has a gyroid solution as a stable equilibrium one in a certain parameter region. In their study, however, the simulations were carried out in a small system where the system size was the equilibrium period of gyroid.

It is known that the spatial period of a gyroid structure is slightly different from that of lamellar and hexagonal structures.[2] Therefore, to study the morphological transitions, one has either to provide a sufficiently large system or to change the system size during transitions. At present, these methods are difficult technically to carry out in three dimensions. Hence we shall apply an alternative approach as is shown in the subsequent sections.

3. Mode Expansion

In the present study, we are mainly concerned with transitions that involve a gyroid structure and apply the mode expansion method by Qi and Wang.[43] Their mode expansion, however, contains only one mode which is insufficient to express a gyroid symmetry. Therefore, we extend the mode expansion method such that a gyroid structure is properly taken into account. The mode expansion approximates that the concentration variation is sinusoidal. This is valid only in the weak segregation limit. It is noted, however, that since a gyroid structure appears in the weak and the intermediate segregation regimes,[2] the mode expansion method is justified in the present investigation where we are concerned with the weak segregation regime.

A gyroid structure can be approximated by the following level surface representation

$$0 = 8(1 - s)[\sin 2x \sin z \cos y + \sin 2y \sin x \cos z + \sin 2z \sin y \cos x] - 4s[\cos 2x \cos 2y + \cos 2y \cos 2z + \cos 2z \cos 2x] - u \tag{6}$$

where s and u are the parameters.[51] Using eq 6, we expand ϕ as

$$\phi(\vec{r}, t) = \bar{\phi} + [\sum_{l=1}^{12} a_l(t) e^{i\vec{q}_l \cdot \vec{r}} + \sum_{m=1}^{6} b_m(t) e^{i\vec{p}_m \cdot \vec{r}} + \sum_{n=1}^{12} c_n(t) e^{i\vec{k}_n \cdot \vec{r}} + \text{c.c.}] \quad (7)$$

where a_l, b_m, and c_n are the real amplitudes and c.c. means complex conjugate. The fundamental reciprocal vectors $\vec{q}_l$ and $\vec{p}_m$ for a gyroid are obtained easily by comparing eq 6 with eq 7 as

$$\begin{aligned}
&\vec{q}_1 = C_Q(2, -1, 1) && \vec{q}_2 = C_Q(-2, 1, 1)\\
&\vec{q}_3 = C_Q(-2, -1, 1) && \vec{q}_4 = C_Q(2, 1, 1)\\
&\vec{q}_5 = C_Q(-1, -2, 1) && \vec{q}_6 = C_Q(1, -2, 1)\\
&\vec{q}_7 = C_Q(-1, 2, 1) && \vec{q}_8 = C_Q(1, 2, 1)\\
&\vec{q}_9 = C_Q(1, -1, -2) && \vec{q}_{10} = C_Q(1, 1, -2)\\
&\vec{q}_{11} = C_Q(-1, 1, -2) && \vec{q}_{12} = C_Q(-1, -1, -2)\\
&\vec{p}_1 = C_P(2, 2, 0) && \vec{p}_2 = C_P(2, -2, 0)\\
&\vec{p}_3 = C_P(0, 2, 2) && \vec{p}_4 = C_P(0, -2, 2)\\
&\vec{p}_5 = C_P(2, 0, 2) && \vec{p}_6 = C_P(-2, 0, 2)
\end{aligned} \quad (8)$$

where the coefficients are chosen as $C_Q = Q/\sqrt{6}$, $C_P = P/(2\sqrt{2})$ so that $|\vec{q}_i| = Q$ and $|\vec{p}_i| = P$. We note the relation

$$Q^2 = \frac{3}{4}P^2 \quad (9)$$

so that $C_Q = C_P$. In the spirit of the mode expansion, we shall impose the relation 9 not only in equilibrium but also during the structural transition. The reciprocal lattice vectors for c_n in eq 7 are given by

$$\begin{aligned}
\vec{k}_1 &= C_Q(-w, -w + 1, w + 1)\\
\vec{k}_2 &= C_Q(w - 1, w + 1, w)\\
\vec{k}_3 &= C_Q(w, -w - 1, w - 1)\\
\vec{k}_4 &= C_Q(-w + 1, w, w + 1)\\
\vec{k}_5 &= C_Q(-w, w + 1, w - 1)\\
\vec{k}_6 &= C_Q(w, w - 1, w + 1)\\
\vec{k}_7 &= C_Q(-w - 1, -w, w - 1)\\
\vec{k}_8 &= C_Q(w - 1, -w, w + 1)\\
\vec{k}_9 &= C_Q(w + 1, -w + 1, w)\\
\vec{k}_{10} &= C_Q(w + 1, w, w - 1)\\
\vec{k}_{11} &= C_Q(-w - 1, w - 1, w)\\
\vec{k}_{12} &= C_Q(-w + 1, -w - 1, w)
\end{aligned} \quad (10)$$

where $w = 2\sqrt{3}/3$. In a previous paper,[47] we did not introduce the modes c_n. However, to investigate the transitions LAM ↔ BCC and HEX ↔ BCC, the amplitudes a_l and b_m are insufficient. In fact, if only a_1 is finite, then it expresses a lamellar structure, and if a_2, a_6, and a_{10}, for example, are finite with the same magnitude, it expresses a hexagonal structure. A BCC structure is obtained, e.g., if only a_1, a_7, a_{12}, c_1, c_7, and c_{12} are not zero with the same magnitude.

A gyroid structure is expressed as $|a_l| = a_G \neq 0$, $|b_m| = b_G \neq 0$ ($l = 1, ..., 12$; $m = 1, ..., 6$), and $c_n = 0$ ($n = 1, ..., 12$). If one defines the isosurface given by $\phi = 0$, the constants a_G, b_G, and $\bar{\phi}$ are related to s and u in eq 6 as $a_G = c(1 - s)$, $b_G = -cs$, and $\bar{\phi} = -cu$ with an arbitrary constant c.

It is noted that the vectors shown in eqs 8 and 10 are not independent but satisfy some relations. Several examples are listed as

$$\begin{aligned}
\vec{q}_1 - \vec{q}_4 + \vec{q}_{11} - \vec{q}_{12} &= 0\\
\vec{q}_2 + \vec{q}_7 + \vec{q}_9 + \vec{p}_2 &= 0\\
\vec{q}_1 - \vec{q}_3 - \vec{p}_1 - \vec{p}_2 &= 0\\
\vec{q}_1 + \vec{q}_7 - \vec{k}_1 + \vec{k}_7 &= 0\\
\vec{q}_6 - \vec{p}_5 + \vec{k}_3 - \vec{k}_9 &= 0\\
\vec{p}_1 - \vec{p}_2 - \vec{p}_3 + \vec{p}_4 &= 0\\
\vec{k}_2 - \vec{k}_9 - \vec{k}_{11} - \vec{k}_{12} &= 0\\
\vec{q}_1 + \vec{q}_7 + \vec{q}_{12} &= 0\\
\vec{q}_2 + \vec{q}_4 - \vec{p}_3 &= 0\\
\vec{q}_4 - \vec{k}_4 + \vec{k}_{11} &= 0\\
\vec{p}_2 + \vec{p}_3 - \vec{p}_5 &= 0
\end{aligned} \quad (11)$$

Substituting eq 7 into eq 5 and ignoring the higher harmonics, which is justified in the weak segregation limit, we obtain a coupled set of equations for the amplitudes. For example, equation for a_1 is given by

$$\begin{aligned}
\frac{da_1}{dt} = (-Q^4 + \tau Q^2 - \alpha)a_1 - gQ^2[3(\bar{\phi}^2 - {a_1}^2)a_1 + 6(\sum_{l=1}^{12} {a_l}^2 + \sum_{m=1}^{6} {b_m}^2 + \sum_{n=1}^{12} {c_n}^2)a_1 + 6(\bar{\phi}a_3b_4 + \bar{\phi}a_7a_{12} + \bar{\phi}c_7c_{12} + a_1b_2b_5 + a_2a_3a_4 + a_2a_5a_8 + a_2a_6a_7 + a_3b_1b_2 + a_3b_1b_5 + a_3b_2b_6 + a_3b_5b_6 + a_4a_9a_{10} + a_4a_{11}a_{12} + a_5a_{10}b_2 + a_5a_{10}b_5 + a_5a_{12}b_6 + a_6a_9b_3 + a_6a_9b_6 + a_6a_{11}b_2 + a_6a_{11}b_4 + a_6a_{11}b_5 + a_7a_{10}b_1 + a_7c_1c_7 + a_8a_9b_4 + a_8a_{11}b_1 + a_8a_{11}b_3 + a_{12}c_1c_{12} + b_4c_8c_9)]
\end{aligned} \quad (12)$$

Equations for other amplitudes are listed in Appendix A. Similarly, the free energy given by eq 2 can also be written in terms of a_l, b_m, c_n, and P as

$$F_{\text{amp}} = F(\{a_l\}, \{b_m\}, \{c_n\}, P) \quad (13)$$

The explicit form is given in Appendix B. It is mentioned here that we have developed a special algorithm to derive the amplitude equations and the free energy to avoid arithmetic errors during the tedious manipulation.

Since the spatial period of gyroid is different from that of other structures, we have to take account of the time evolution of the period during transitions. At present, we have no systematic way to derive the equation for P (or Q). Here we employ the relaxation dynamics for the

wavenumber:

$$\frac{dP^2}{dt} = -h\frac{\partial F_{amp}}{\partial P^2} = -h\left[\left(\frac{3}{4} - \frac{4\alpha}{3P^4}\right)\left(\sum_{l=1}^{12} a_l^2 + \sum_{n=1}^{12} c_n^2\right) + \left(1 - \frac{\alpha}{P^4}\right)\sum_{m=1}^{6} b_m^2\right] \quad (14)$$

where h is a positive constant. It is noted that when the wavenumber is time-dependent, the amplitude equations are generally modified. In fact, there is an additive term like dP/dt on the left-hand side of the amplitude equations (33) in Appendix A. However, we ignore this term, for simplicity, which is valid if h is sufficiently small.

Before closing this section, we make a remark about the approximations used in the mode expansion. First of all, we have not considered the spatial dependence of the amplitudes. Hence, a coexistence of two different phases is not treated in the present theory. Second, we have assumed that the amplitudes are real, omitting the phase degrees of freedom, which describe the elastic effect of the structures. However, our main concern is how domains break up and reconnect during the morphological transitions and what kind of structures appears in the course of transitions. For this purpose, the present method causes no serious limitations.

4. Equilibrium Solutions and Phase Diagram

The stable equilibrium structures are obtained by solving eqs 14 and 33 numerically. The initial conditions are chosen such that $a_l = b_m = c_n = 0$ with small random numbers superimposed. The parameters α and g in the free energy 2 are set to be $\alpha = g = 1$ throughout this paper. The coefficient h in eq 14 is chosen as $h = 1$. In the preceding section we mention that h should be small in the present theory. We have performed simulations for $h = 0.001$ and verified that the results are not much different from the case of $h = 1$.

The four fundamental solutions of lamellar, hexagonal, gyroid, and BCC structures are easily obtained. The phase diagram can be determined by evaluating the free energy of these equilibrium structures given in Appendix B. Figure 1 is the phase diagram in the $\tau-\bar{\phi}$ plane obtained in this way. This phase diagram is qualitatively consistent with that derived previously.[2,3] The equilibrium value of Q of gyroid is given by $Q = Q^* \approx 0.98$ in the present unit of scale, which is slightly smaller than that of other structures $Q^* = 1$. It is emphasized that although this difference of Q^* is quite small, if one omits it, the stable region of G disappears completely in the phase diagram 1. This fact implies that careful simulations are necessary to investigate morphological transitions by solving directly eq 5.

It is noted that there are other stable structures apart from lamellar, hexagonal, BCC, and gyroid structures as listed in Appendix C. However, we have verified that the free energies for other structures are higher and they are only metastable.

Among these metastable solutions, there are two interesting solutions. One is given by the set of $a_2 = a_4 = 0.1655$, $-b_3 = b_4 = 0.02527$, $b_1 = b_2 = b_5 = b_6 = -0.07876$, and $Q^* = 0.9543$ for $\tau = 2.3$ and $\bar{\phi} = -0.05$.

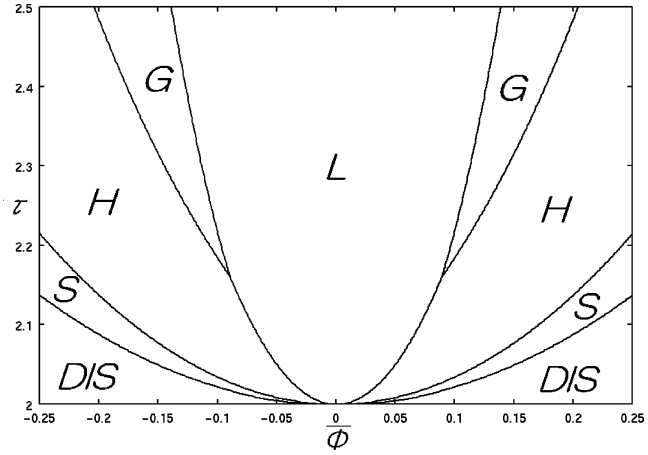

Figure 1. Phase diagram of the $\tau-\bar{\phi}$ plane. The regions indicated by L, H, G, and S are the stable phase of lamellae, hexagons, gyroid, and BCC, respectively. DIS means a disorder phase.

Table 1. First Four Stable Solutions[a]

	I	II	III	IV
a_1	0.0	0.0	0.0	0.0
a_2	0.0	0.0	0.0	0.0
a_3	0.0	0.0	0.0	0.09162
a_4	0.0	0.0	0.0	0.0
a_5	0.0	0.0	0.0	−0.09162
a_6	0.0	0.0	0.0	0.0
a_7	0.0	0.0	0.0	0.0
a_8	0.0	0.0	0.0	0.0
a_9	−0.1054	−0.09450	−0.1673	0.0
a_{10}	0.0	0.0	0.0	0.09162
a_{11}	0.1054	0.09450	0.1673	0.0
a_{12}	0.0	0.0	0.0	0.0
b_1	0.0	0.0	0.0	0.02524
b_2	0.0	−0.05156	0.0	0.0
b_3	0.0	0.0	0.08113	0.0
b_4	0.0	0.0	0.08113	0.02524
b_5	0.0	0.0	0.08113	0.0
b_6	0.0	0.0	0.08113	0.02524
c_1	0.0	0.0	0.0	0.0
c_2	0.0	0.0	0.0	0.0
c_3	0.0	0.0	0.0	0.0
c_4	0.0	0.0	0.0	0.0
c_5	0.0	0.0	0.0	0.0
c_6	0.0	0.0	0.0	0.0
c_7	0.0	0.0	0.0	0.0
c_8	0.0	0.0	0.0	0.0
c_9	0.0	0.0	0.0	0.0
c_{10}	0.0	0.0	0.0	0.0
c_{11}	0.0	0.0	0.0	0.0
c_{12}	0.0	0.0	0.0	0.0
P^2	1.333	1.284	1.216	1.306
τ	2.1	2.1	2.3	2.1
$\bar{\phi}$	0.0	−0.11	0.0	0.0

[a] These exist for finite range of τ and $\bar{\phi}$. The values of these parameters in the table are only representative.

This is one example of the combination of the amplitudes. There are several other sets which produce the same symmetry. Hereafter, we will call this structure an intermediate structure (IM). The Bragg points are shown in Figure 2 in the reciprocal lattice space. Note that a nonproper hexagon (indicated by the red spheres) is constituted, below and above which four Bragg points (white spheres) with a rectangular symmetry are formed. The location of these four points is given by translation of the four points of the hexagon. The other is the solution given by the set of the amplitudes, e.g., $a_1 = -a_3 = -0.04998$, $a_7 = -a_8 = -a_9 = -a_{12} = 0.1367$, $b_4 =$

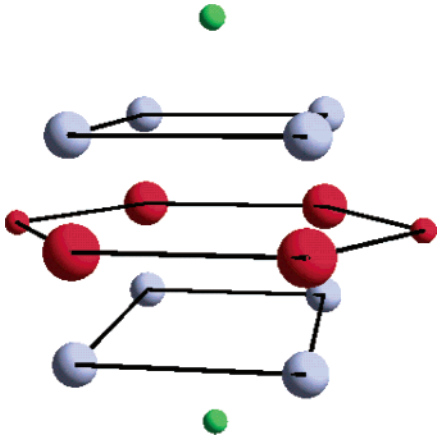

Figure 2. Bragg points of the intermediate structure in the reciprocal lattice space. The radius of the spheres indicates the relative peak intensity. In this figure and in Figure 3, the Bragg point at the origin which is the center of the hexagon is removed for the sake of clarity. The Bragg points on the same plane are connected with lines. It is noted that the quasi-proper hexagon and the two rectangles are parallel to each other.

Table 2. Second Four Stable Solutions

	V	VI	VII	VIII
a_1	−0.08165	0.006924	−0.06523	−0.04428
a_2	0.08165	0.0	0.06523	0.04428
a_3	0.0	0.09127	0.06523	0.04428
a_4	0.0	0.0	−0.06523	−0.04428
a_5	0.0	−0.09127	−0.06523	−0.04428
a_6	0.08165	0.0	0.06523	0.04428
a_7	0.08165	−0.006924	0.06523	0.04428
a_8	0.0	0.0	−0.06523	−0.04428
a_9	0.0	0.0	0.0	−0.04428
a_{10}	0.0	0.09127	0.0	0.04428
a_{11}	0.0	0.0	0.0	0.04428
a_{12}	0.0	0.006924	0.0	−0.04428
b_1	0.0	0.02518	0.1405	0.0
b_2	0.0	0.002451	0.1405	0.0
b_3	0.0	0.002451	0.01545	0.0
b_4	0.0	0.02518	0.01545	0.0
b_5	0.0	0.002451	0.01545	0.0
b_6	0.0	0.02518	0.01545	0.0
c_1	0.0	0.0	0.0	0.0
c_2	0.0	0.0	0.0	0.0
c_3	0.0	0.0	0.0	0.0
c_4	0.0	0.0	0.0	0.0
c_5	0.0	0.0	0.0	0.0
c_6	0.0	0.0	0.0	0.0
c_7	0.0	0.0	0.0	0.0
c_8	0.0	0.0	0.0	0.0
c_9	0.0	0.0	0.0	0.0
c_{10}	0.0	0.0	0.0	0.0
c_{11}	0.0	0.0	0.0	0.0
c_{12}	0.0	0.0	0.0	0.0
P^2	1.333	1.306	1.141	1.333
τ	2.2	2.1	2.3	2.1
$\bar{\phi}$	0.0	−0.01	0.0	0.0

0.03865, and $Q^* = 0.9973$ for $\tau = 2.3$ and $\bar{\phi} = -0.05$. This is identified with the *Fddd* structure. The Bragg points of this structure are shown in Figure 3. This has also a quasi-proper hexagon indicated by the red spheres and is quite similar to the IM structure except for the fact that the rectangle (constituted by the white spheres) is smaller than that in Figure 2. We shall return to these structures in section 6 since *Fddd* structure is formed during the order−order transitions. We have verified numerically that the *Fddd* structure has a lower free energy than IM structure (but, of course, larger than G, HEX, LAM, and BCC) for most parameters in the phase diagram 1. For example, Figure 4 shows the free

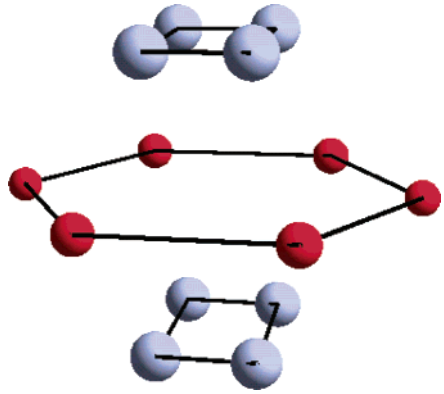

Figure 3. Bragg points of *Fddd* structure in the reciprocal lattice space. Other details are the same as those in Figure 2.

Table 3. Last Four Stable Solutions

	IX	X	XI	XII
a_1	−0.06456	0.047 09	0.0	0.0
a_2	0.064 56	0.069 21	0.0	0.0
a_3	0.064 56	0.098 94	0.0	0.0
a_4	−0.06456	−0.06921	0.0	0.0
a_5	−0.06456	−0.09894	0.0	0.0
a_6	0.064 56	0.069 21	0.0	0.0
a_7	0.064 56	−0.04709	0.0	0.0
a_8	−0.06456	−0.06921	0.0	0.0
a_9	−0.003314	−0.06921	0.0	0.0
a_{10}	0.003314	0.098 94	0.0	0.002473
a_{11}	0.003314	0.069 21	0.0	0.0
a_{12}	−0.003314	0.047 09	−0.1211	−0.1467
b_1	0.1414	−0.01485	0.072 96	0.1014
b_2	0.1414	0.069 82	0.0	0.0
b_3	0.015 19	0.069 82	0.0	0.0
b_4	0.015 19	−0.01485	0.0	0.0
b_5	0.015 19	0.069 82	0.0	0.0
b_6	0.015 19	−0.01485	0.0	0.0
c_1	0.0	0.0	0.0	0.0
c_2	0.0	0.0	0.0	0.0
c_3	0.0	0.0	0.0	0.0
c_4	0.0	0.0	0.0	0.0
c_5	0.0	0.0	0.0	0.0
c_6	0.0	0.0	0.1211	0.1474
c_7	0.0	0.0	0.0	0.0
c_8	0.0	0.0	0.0	0.0
c_9	0.0	0.0	0.0	0.0
c_{10}	0.0	0.0	0.1211	0.1474
c_{11}	0.0	0.0	0.0	0.0
c_{12}	0.0	0.0	0.0	0.0
P^2	1.138	1.262	1.292	1.279
τ	2.3	2.3	2.2	2.3
$\bar{\phi}$	−0.01	0.0	0.0	−0.01

energy of lamellar, gyroid, *Fddd*, and IM structures for $\tau = 2.3$.

We emphasize that the bicontinuous structure which was found previously by solving eq 5 directly in three dimensions[45] and was identified erroneously with a rhombohedral structure has essentially the same Bragg points as the *Fddd* structure in Figure 3. Saeki has also carried out numerical simulations of eq 5 by using an efficient algorithm to relax rapidly to equilibrium[52] and has obtained a bicontinuous structure having a *Fddd* symmetry shown in Figure 3. These facts confirm partially the consistency of the present mode expansion method with the direct simulations of the time evolution equation (5).

It is noted that neither the rhombohedral structure having $R\bar{3}c$ symmetry nor the so-called perforated lamellar structure is a stable solution of the amplitude equations.

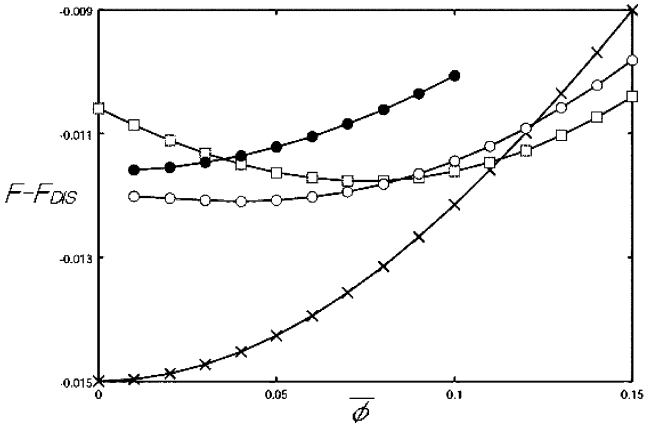

Figure 4. Free energy of lamellar (×), gyroid (square), IM (black circle), and *Fddd* (white circle) structures for $\tau = 2.3$ where F_{DIS} is the free energy for the disorder phase. The lines for *Fddd* and IM are terminated at some values of $\bar{\phi}$, beyond which these stable solutions do not exist.

5. Order−Disorder Transition

Now we study kinetics of the morphological transitions from a disorder state at high temperature to the microphase-separated state. We solve numerically the amplitude equations starting with the initial conditions $a_l = b_m = c_n = 0$ with small random numbers superimposed. The parameters τ and $\bar{\phi}$ are chosen such that lamellar, hexagonal, BCC, and gyroid structures are formed asymptotically. In this and the next sections we carry out numerical simulations of the amplitude equations by adding fluctuating thermal noises since the morphological transitions are first order. The random force is a Gaussian white noise with the variance σ, the value of which is different in the respective case.

Results of numerical simulations are displayed in three different ways: (a) time evolution of the amplitudes, (b) time evolution of the free energy, and (c) domain evolution where the isosurface of $\phi = \phi_{ISO}$ with ϕ_{ISO} constant is represented.

Figure 5 shows formation of a lamellar structure for $\tau = 2.5$ and $\bar{\phi} = -0.07$ starting from the disorder state. The variance of the random force is chosen as $\sigma = 1.39 \times 10^{-5}$ throughout this section. It is found that although only the amplitude $c_2 = -0.4022$ corresponding to a lamellar symmetry evolves asymptotically, some other amplitudes become finite transiently during the ordering process. In particular, we observe an interesting structure around $t = 30$ in Figure 5c where the amplitudes a_2 (≈0.02), a_6, a_{10}, c_2, c_6, and c_{10} are finite. This is essentially a BCC symmetry. By a closer look, we note that there are holes in each lamellae, which constitute a hexagonal lattice within each domain. The three-dimensional configuration of the holes is equivalent with a close-packed structure of spheres. Therefore, this is identical with the so-called perforated lamellar structure.[43,44] As mentioned in the preceding section, however, this structure is not a stable solution of the amplitude equations, and hence one may conclude that this appears only transiently.

A transition from a disorder state to a hexagonal structure is shown in Figure 6 for $\tau = 2.1$ and $\bar{\phi} = -0.15$. The final nonzero amplitudes are given by $a_1 = -a_7 = a_{12} = -0.08538$. In Figure 6c, no structure is drawn at $t = 0$. This is because the isosurface is chosen as $\phi_{ISO} = -0.05$. It is noted that BCC structure appears in themiddle of the transition process. As shown in Figure

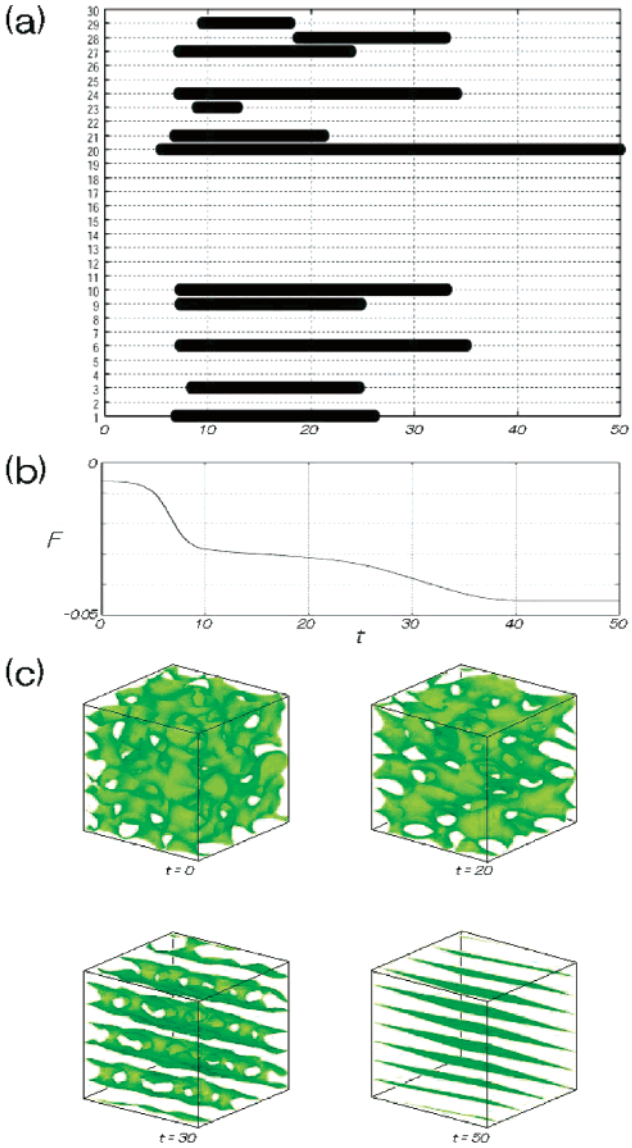

Figure 5. Structural evolution from a disorder state to a lamellar structure for $\bar{\phi} = -0.07$ and $\tau = 2.5$. (a) Time evolution of the amplitudes. The numbers (1, ..., 30) of the vertical axis correspond to a_1, ..., a_{12}, b_1, ..., b_6, and c_1, ..., c_{12}, respectively. The thick black lines are drawn when the absolute value of the amplitudes is larger than 0.05. (b) Time evolution of the free energy during the ordering process. (c) Morphological evolution in the isosurface representation with $\phi_{ISO} = -0.1$.

6a, the amplitudes a_1, a_7, a_{12}, c_1, c_7, and c_{12} dominate others until about $t = 950$, and then c_1, c_7, and c_{12} disappear to form the final hexagonal morphology. This is also clear in Figure 6c.

It is mentioned that the appearance of BCC as an intermediate state occurs only when the system is quenched near the phase boundary between HEX and BCC. A similar phenomenon has been observed in experiments of triblock copolymers.[30]

Finally, we show in Figure 7 that a gyroid structure really appears starting from a disorder state. The parameters are set to be $\tau = 2.4$ and $\bar{\phi} = -0.14$. The amplitudes of the final gyroid structure are $a_1 = a_4 = a_5 = a_8 = a_{10} = a_{11} = 0.09085$, $a_2 = a_3 = a_6 = a_7 = a_9 = a_{12} = -0.09085$, $b_j = -0.04102$ ($j = 1, ..., 6$), and $c_k = 0$ ($k = 1, ..., 12$).

We have shown the results of the ordering from DIS to LAM, HEX, and G structures but do not show the

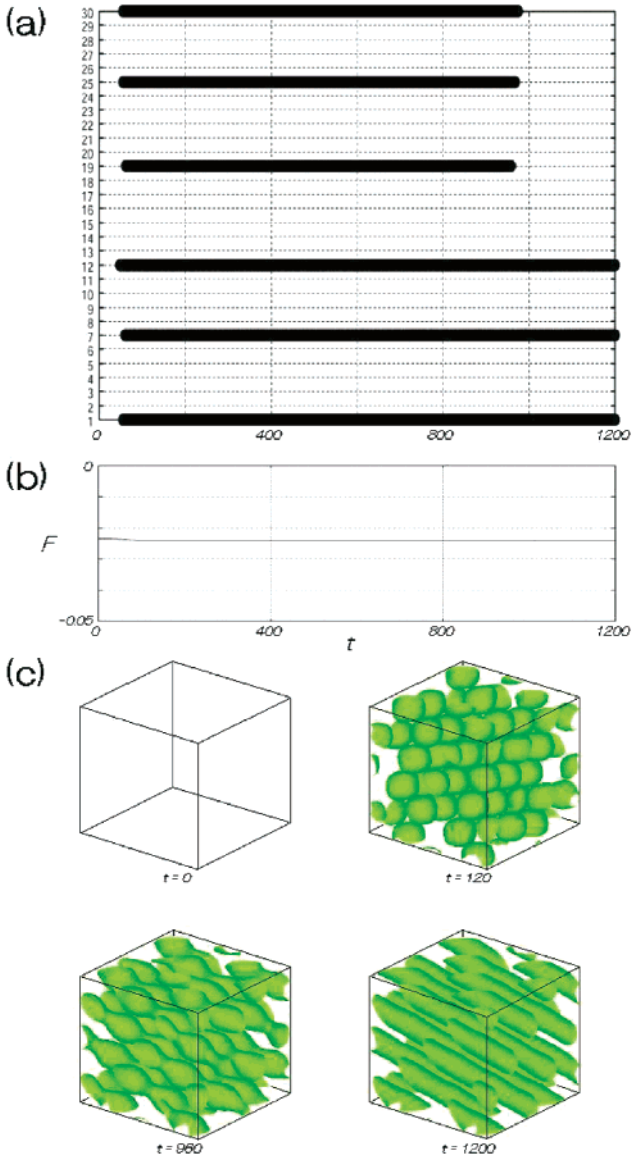

Figure 6. Structural evolution from a disorder state to a hexagonal structure for $\bar{\phi} = -0.15$ and $\tau = 2.2$. (a) Time evolution of the amplitudes. The numbers (1, ..., 30) of the vertical axis correspond to a_1, ..., a_{12}, b_1, ..., b_6, and c_1, ..., c_{12}, respectively. The thick black lines are drawn when the absolute value of the amplitudes is larger than 0.03. (b) Time evolution of the free energy during the ordering process. (c) Morphological evolution in the iso-surface representation with $\phi_{ISO} = -0.05$.

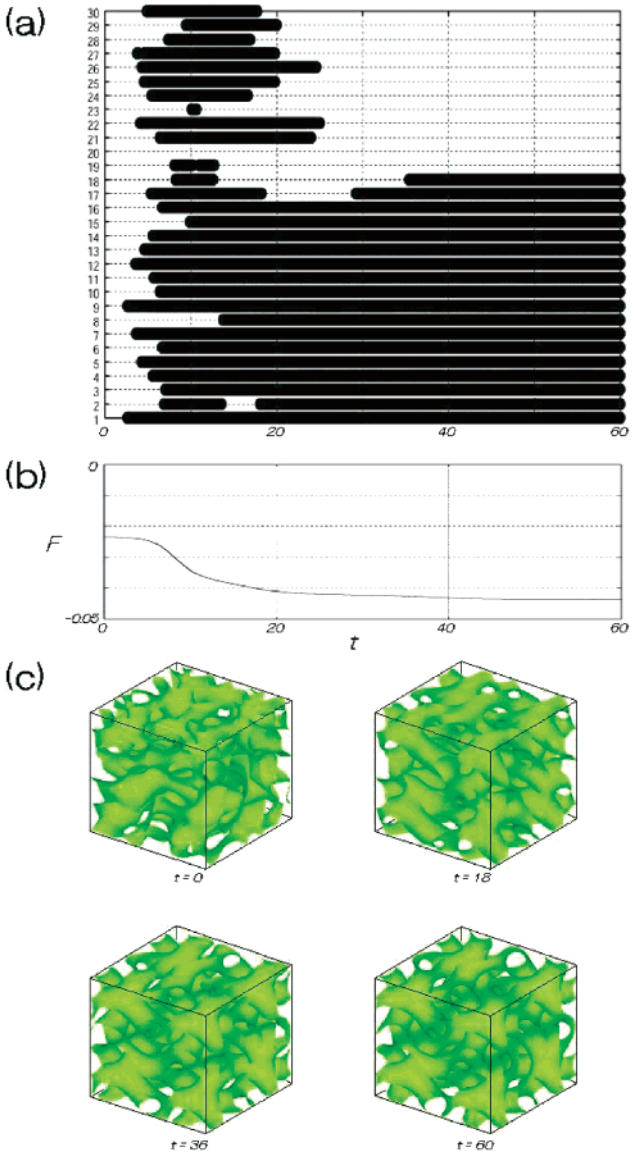

Figure 7. Structural evolution from a disorder state to a gyroid structure for $\bar{\phi} = -0.14$ and $\tau = 2.4$. (a) Time evolution of the amplitudes. The numbers (1, ..., 30) of the vertical axis correspond to a_1, ..., a_{12}, b_1, ..., b_6, and c_1, ..., c_{12}, respectively. The thick black lines are drawn when the absolute value of the amplitudes is larger than 0.01. (b) Time evolution of the free energy during the ordering process. (c) Morphological evolution in the isosurface representation with $\phi_{ISO} = -0.14$.

transition from DIS to BCC since nothing particular is found in this case.

6. Order−Order Transition

In this section, the OOTs are investigated numerically. The ordered states obtained in section 5 are used as the initial conditions.

Figure 8 shows the structural transition from gyroid to a hexagonal structure. Initially we provide a gyroid structure for $\tau = 2.5$ and $\bar{\phi} = -0.17$ and then change the value of τ to $\tau = 2.2$. The initial values of the amplitudes are $a_1 = a_4 = a_5 = a_8 = a_9 = a_{12} = -0.1013$, $a_2 = a_3 = a_6 = a_7 = a_{10} = a_{11} = 0.1013$, $b_i = -0.04733$ ($i = 1$, ..., 6), and $c_j = 0$ ($j = 1$, ..., 12). The final nonzero amplitudes for the hexagonal structure are found to be $a_1 = -a_7 = a_{12} = -0.1273$. This means that the cylidrical axis of the hexagons is parallel to the (1, 1, −1) direction. In Figure 8a, the time evolution of a_i and b_j is displayed ($i = 1$, ..., 12; $j = 1$, ..., 6). The variance of the random force is chosen as $\sigma = 8.89 \times 10^{-4}$. It is found that the morphological change is not gradual but abrupt after an induction period. In fact, the amplitudes other than a_1, a_7, and a_{12} disappear at about $t = 1800$. This sudden change of the structure is also clearly seen in the variation of the free energy in Figure 8b.

The morphological transition from gyroid to a lamellar structure is shown in Figure 9 where $\bar{\phi} = -0.1$ and τ is changed from $\tau = 2.2$ to 2.5. The initial amplitudes are set to be $a_1 = a_4 = a_5 = a_8 = a_9 = a_{12} = -0.06456$, $a_2 = a_3 = a_6 = a_7 = a_{10} = a_{11} = 0.06456$, $b_i = -0.02353$ ($i = 1$, ..., 6), and $c_j = 0$ ($j = 1$, ..., 12). The final nonzero amplitude for the lamellar structure is $a_4 = -0.3958$. The variance of the random force is chosen as $\sigma = 2.4 \times 10^{-2}$. There are several interesting properties in this

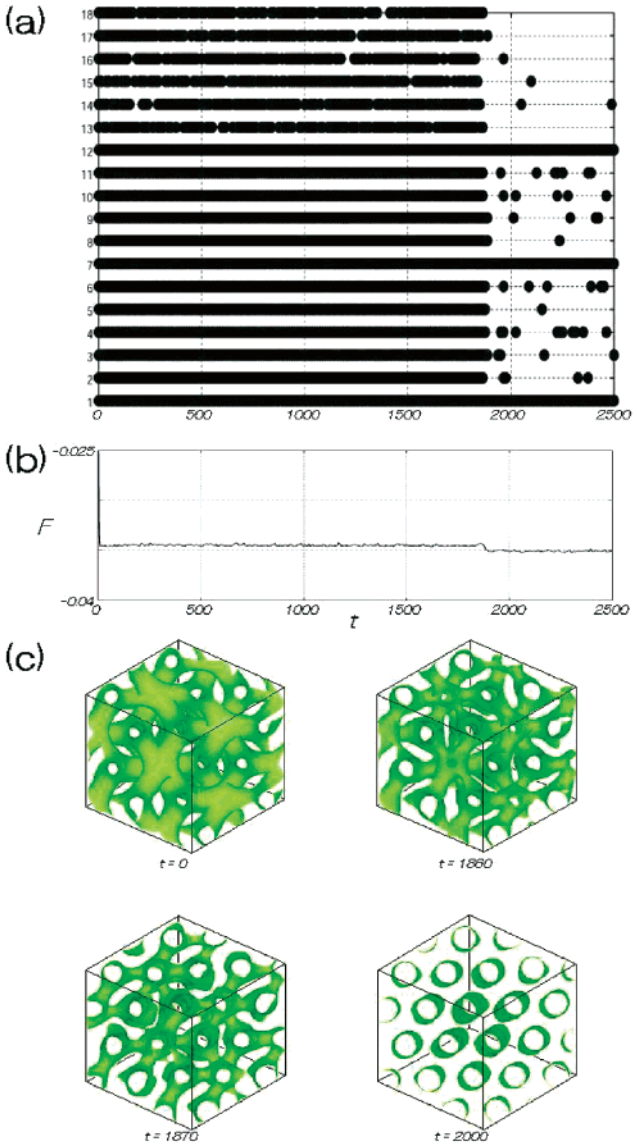

Figure 8. Structural evolution from gyroid for $\bar{\phi} = -0.17$ and $\tau = 2.5$ to a hexagonal structure for $\bar{\phi} = -0.17$ and $\tau = 2.2$. (a) Time evolution of the amplitudes. The numbers (1, ..., 18) of the vertical axis correspond to a_1, ..., a_{12} and b_1, ..., b_6, respectively. The thick black lines indicate that the absolute value of the amplitudes is larger than 0.015. In this figure and Figures 9a, 12a, and 13a, the amplitudes c_k ($k = 1$, ..., 12) are not displayed because these values are extremely small. Random black points after $t = 1800$ arise from the fluctuation of the amplitudes due to the random force. (b) Variation of the free energy from gyroid to a hexagonal structure. (c) Morphological evolution in the isosurface representation with $\phi_{ISO} = -0.1$.

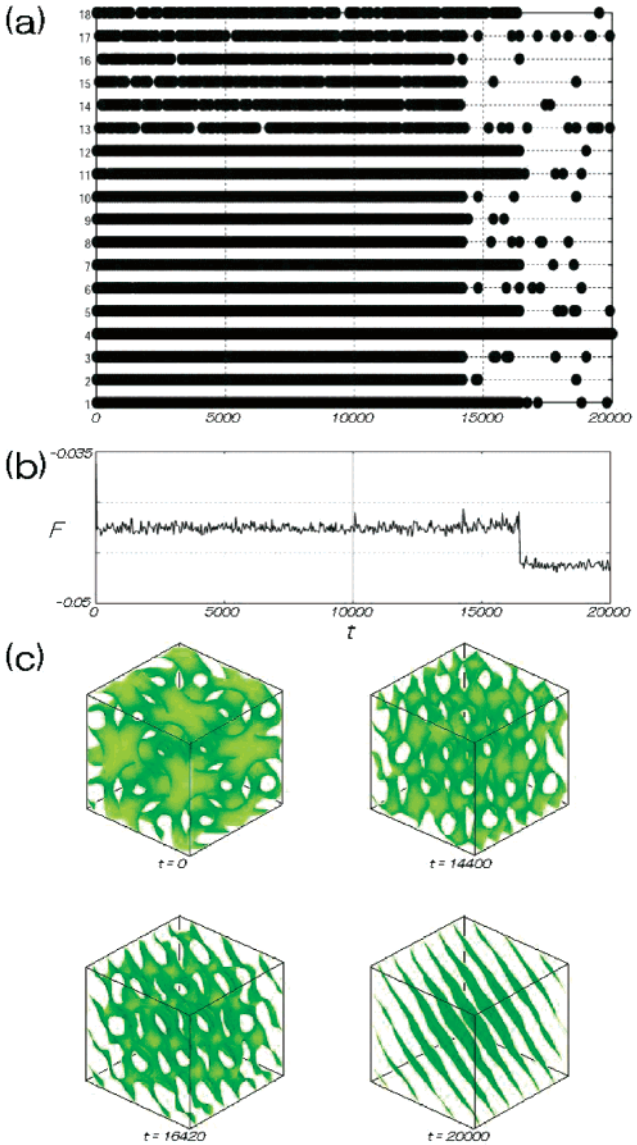

Figure 9. Structural evolution from gyroid for $\bar{\phi} = -0.1$ and $\tau = 2.2$ to a lamellar structure for $\bar{\phi} = -0.1$ and $\tau = 2.5$. (a) Time evolution of the amplitudes. The numbers (1, ..., 18) of the vertical axis correspond to a_1, ..., a_{12} and b_1, ..., b_6, respectively. The thick black lines indicate that the absolute value of the amplitudes is larger than 0.03. (b) Time evolution of the free energy from gyroid to a lamellar structure. (c) Morphological evolution in the isosurface representation with $\phi_{ISO} = -0.1$.

transition. First of all, one finds that the transition from gyroid to a lamellar structure is quite slow compared with that from gyroid to a hexagonal structure in Figure 8. The initial gyroid structure persists for a long period up to about $t = 14\,200$ and then changes to another structure given by $a_1 = a_4 = -a_{11} = a_{12} = -0.1730$, $a_5 = -a_7 = -0.07918$, and $b_6 = 0.05970$. Other amplitudes are vanishingly small. After staying in the intermediate state, it changes to the final lamellar structure. As can be seen in Figure 9a, this structure appears between about $t = 14\,000$ and about $t = 17\,000$. After $t = 17\,000$, it changes to the final lamellar structure. As shown in Figure 9b, the free energy does not change appreciably in the transition from gyroid to the intermediate structure, indicating that this metastable state has almost the same free energy as that of a gyroid structure for this set of parameters.

It is emphasized that this intermediate structure is essentially identical to the *Fddd* structure discussed in section 4. The corresponding Bragg points are completely consistent with those shown in Figure 3. The domain pattern of this structure in various directions is shown in Figure 10. For instance, Figure 10c is the domain pattern viewing from the direction normal to the plane constituted by the quasi-proper hexagonal Bragg points in Figure 3.

The structural transition from gyroid to BCC structure is shown in Figure 11. We provide gyroid for $\tau = 2.5$ and $\bar{\phi} = -0.16$ and then change the parameter to $\tau = 2.07$. The initial values of the amplitudes are $a_1 = a_4 = a_5 = a_8 = a_9 = a_{12} = -0.1014$, $a_2 = a_3 = a_6 = a_7 = a_{10}$

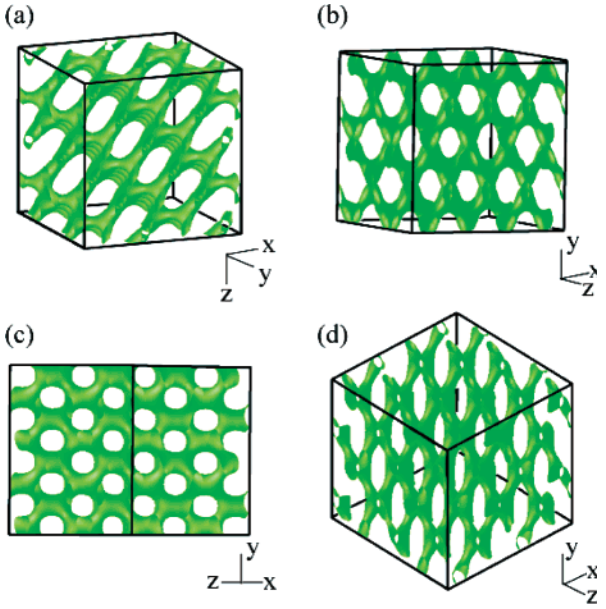

Figure 10. Domain morphologies of the *Fddd* structure. The direction of the orthogonal coordinates is shown on the lower right of each figure.

$= a_{11} = 0.1014$, $b_i = -0.04776$ ($i = 1, ..., 6$), and $c_j = 0$ ($j = 1, ..., 12$). The final nonzero amplitudes of the BCC structure are given by $a_1 = -a_7 = a_{12} = c_1 = -c_7 = c_{12} = -0.03877$. The variance of the random force is chosen as $\sigma = 1.39 \times 10^{-5}$. In Figure 11a,b we show the time evolution of a_i, b_j, c_k ($i, k = 1, ..., 12$; $j = 1, ..., 6$) and the free energy. We note that there are four stages in this transition process. Just after changing the parameter τ, all the amplitudes b_j vanish rapidly leaving the amplitudes a_i. This continues until around $t = 100$, and then only a_1, a_7, and a_{12} survive corresponding to a hexagonal structure. At about $t = 220$, the amplitudes c_1, c_7, and c_{12} grow so that the final BCC structure emerges. Except for the initial stage, the free energy change is quite small.

The morphological transition from a lamellar structure to a gyroid structure is investigated for $\bar{\phi} = -0.13$ and by changing τ from $\tau = 2.5$ to $\tau = 2.4$. The results are shown in Figure 12. The nonzero amplitude for the initial lamellar structure is $a_7 = 0.3870$, and the final amplitudes for the gyroid structure are $a_1 = a_2 = a_7 = a_8 = a_{11} = a_{12} = 0.09086$, $a_3 = a_4 = a_5 = a_6 = a_9 = a_{10} = -0.09086$, $b_i = -0.04113$ ($i = 1, ..., 6$), and $c_j = 0$ ($j = 1, ..., 12$). The variance of the random force is chosen as $\sigma = 1.013 \times 10^{-2}$. In this transition, there appears a long induction period, which follows a short interval of a hexagonal phase with $a_1 = a_7 = a_{12} = 0.1808$ and then change to the same *Fddd* structure as in Figure 10 at about $t = 16000$. This structure has nonzero amplitudes given by $a_1 = -a_4 = a_{11} = a_{12} = 0.1517$, $a_5 = -a_7 = -0.07903$, and $b_6 = 0.04653$. The emergence of the *Fddd* structure here seems strange somehow. In fact, as is seen in Figure 12b, the free energy in the *Fddd* stage is slightly larger than those of lamellar and gyroid structures. However, here we have used the random forces as small as possible. If the magnitude of the random force were smaller, no transition would occur within accessible simulation time.

The morphological transition from a hexagonal structure to a gyroid structure is shown in Figure 13, where $\bar{\phi} = -0.16$ and τ is changed from $\tau = 2.2$ to 2.5. The initial nonzero amplitudes are set to be $a_1 = -a_7 = a_{12}$

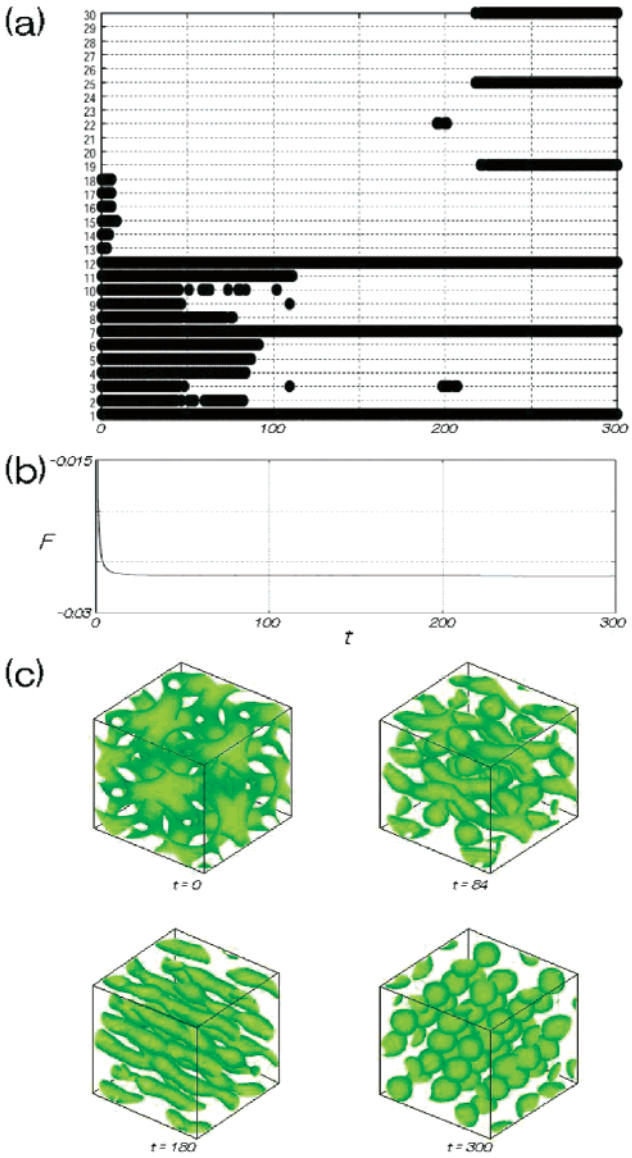

Figure 11. Structural evolution from gyroid for $\bar{\phi} = -0.16$ and $\tau = 2.5$ to a BCC structure for $\bar{\phi} = -0.16$ and $\tau = 2.07$. (a) Time evolution of the amplitudes. The numbers (1, ..., 30) of the vertical axis correspond to a_1, ..., a_{12}, b_1, ..., b_6, and c_1, ..., c_{12}, respectively. The thick black lines indicate that the absolute value of the amplitudes is larger than 0.015. (b) Time evolution of the free energy. (c) Morphological evolution in the isosurface representation with $\phi_{ISO} = -0.05$.

$= -0.1281$, and the final nonzero amplitudes are $a_1 = a_2 = a_5 = a_6 = a_{11} = a_{12} = -0.1014$, $a_3 = a_4 = a_7 = a_8 = a_9 = a_{10} = 0.1014$, and $b_i = -0.04776$ ($i = 1, ..., 6$). The variance of the random force is chosen as $\sigma = 1.61 \times 10^{-2}$. As is seen from Figure 13c, an *Fddd* structure having the amplitudes $a_1 = -a_4 = a_{11} = a_{12} = -0.1680$, $a_5 = -a_7 = -0.09092$, and $b_6 = 0.05179$ appears only for short instant near $t \approx 3000$ after a long induction period.

The morphological transition from a BCC to a gyroid structure is shown in Figure 14, where $\bar{\phi} = -0.16$ and τ is changed from $\tau = 2.07$ to 2.5. The initial nonzero amplitudes for the BCC structure are $-a_1 = a_7 = -a_{12} = -c_1 = c_7 = -c_{12} = 0.03877$, and the final nonzero amplitudes for the gyroid structure are $a_1 = a_2 = a_5 = a_6 = a_{11} = a_{12} = 0.1014$, $a_3 = a_4 = a_7 = a_8 = a_9 = a_{10} = -0.1014$, and $b_i = -0.04776$ ($i = 1, ..., 6$). The variance of the random force is chosen as $\sigma = 1.39 \times 10^{-2}$. The

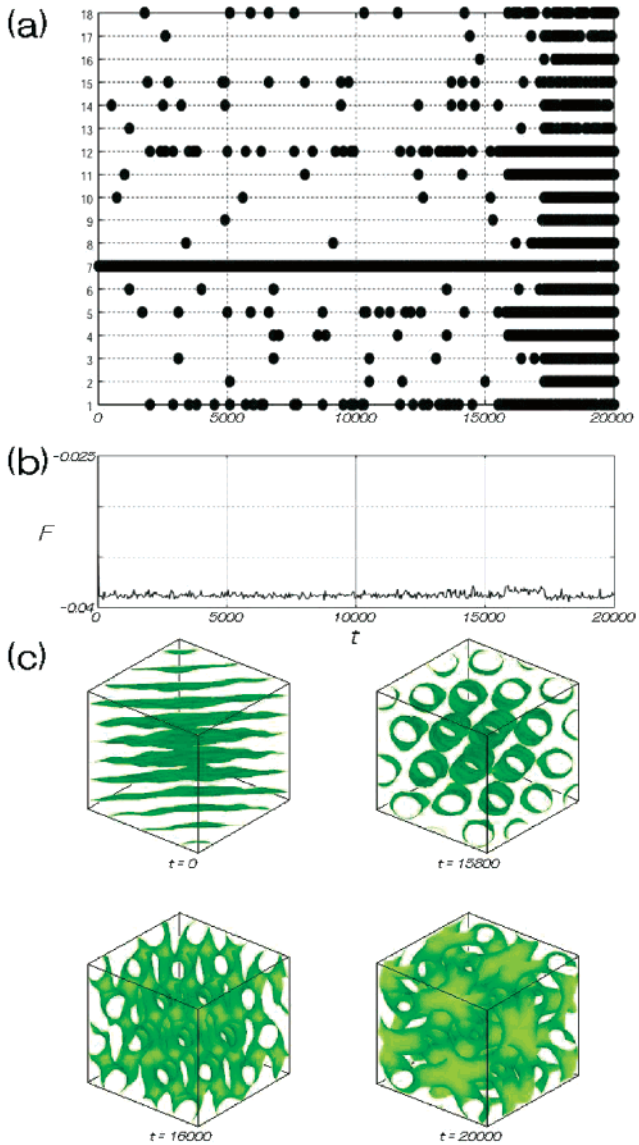

Figure 12. Structural evolution from a lamellar for $\bar{\phi} = -0.13$ and $\tau = 2.5$ to a gyroid structure for $\bar{\phi} = -0.13$ and $\tau = 2.4$. (a) Time evolution of the amplitudes. The numbers (1, ..., 18) of the vertical axis correspond to a_1, ..., a_{12} and b_1, ..., b_6, respectively. The thick black lines indicate that the absolute value of the amplitudes is larger than 0.03. (b) Time evolution of the free energy. (c) Morphological evolution in the isosurface representation with $\phi_{ISO} = -0.1$.

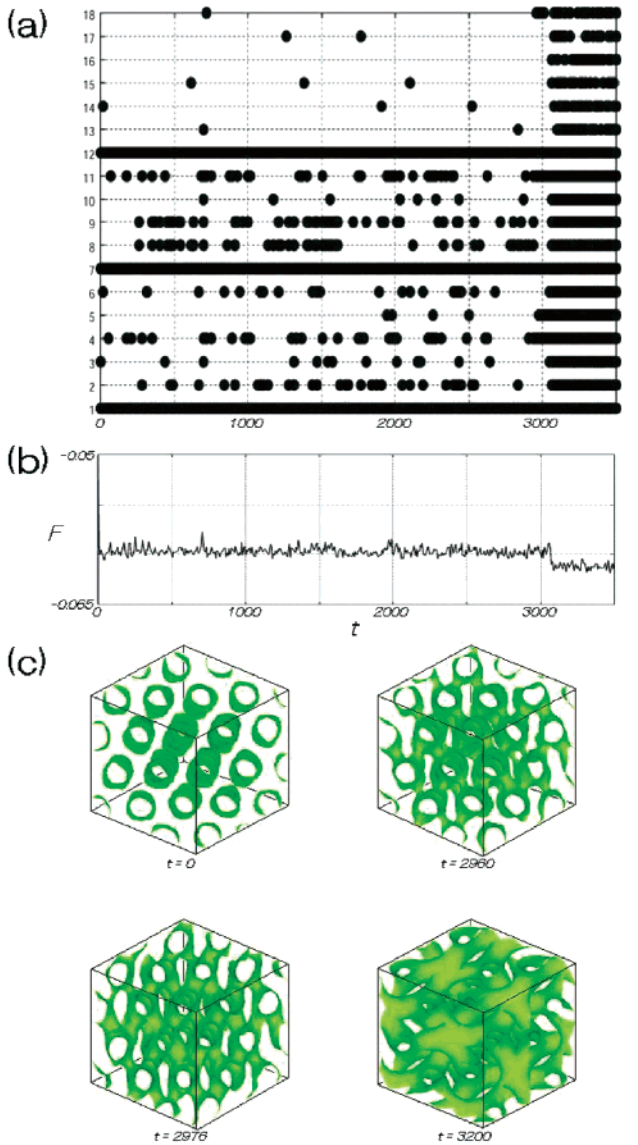

Figure 13. Structural evolution from a hexagonal for $\bar{\phi} = -0.16$ and $\tau = 2.2$ to a gyroid structure for $\bar{\phi} = -0.16$ and $\tau = 2.5$. (a) Time evolution of the amplitudes. The numbers (1, ..., 18) of the vertical axis correspond to a_1, ..., a_{12} and b_1, ..., b_6, respectively. The thick black lines indicate that the absolute value of the amplitudes is larger than 0.035. (b) Time evolution of the free energy. (c) Morphological evolution in the isosurface representation with $\phi_{ISO} = -0.1$.

BCC structure is quickly destabilized just after changing the parameter τ. A hexagonal structure with $a_1 = -a_7 = a_{12} = -0.2030$ appears, and it lasts until $t = 3000$. Between the hexagonal stage and the final gyroid stage an $Fddd$ structure appears for a short interval. The amplitudes of the $Fddd$ structure are $a_1 = -a_4 = a_{11} = a_{12} = -0.1680$, $a_5 = a_7 = -0.09092$, and $b_6 = 0.05179$.

Before closing this section, we make a remark about the strength of the random force employed in this section. We have used the random forces with larger values of the variance in the transition G → LAM compared to the transition G → HEX in order to trigger the transitions within accessible simulation time. At first sight, this seems strange since the lamellar structure exists in a lower temperature. However, this is not unreasonable if the (free) energy barrier in those first-order transitions becomes higher in lower temperature.

7. Linear Stability of Lamellar Structure

In this section, we discuss a linear stability of a lamellar structure. The main purpose is to understand the fact that a hexagonal structure appears during the transition from LAM to G, as has been shown in Figure 12.

We provide a lamellar structure given by $a_1 = a \neq 0$ and $P^2 = 4\sqrt{\alpha}/3$. Other amplitudes are set to be zero. The equilibrium amplitude a^2 is given by

$$a^2 = \frac{1}{3g\sqrt{\alpha}}(\tau\sqrt{\alpha} - 3g\bar{\phi}^2\sqrt{\alpha} - 2\alpha) \qquad (15)$$

This requires

$$\tau > 3g\bar{\phi}^2 + 2\sqrt{\alpha}$$

In the following analysis, we consider the case where the above condition is satisfied.

The linear stability of the lamellar solution can be examined by substituting $a_1 = a + \delta a_1$, $a_i = \delta a_i$ ($i = 2$, ..., 12), $b_j = \delta b_j$ ($j = 1$, ..., 6), $c_k = \delta c_k$ ($k = 1$, ..., 12), and $P^2 = 4\sqrt{\alpha}/3 + \delta P$ into the amplitude equations and retaining only the linear terms of the deviations:

$$\frac{d\delta a_1}{dt} = -6ga^2\sqrt{\alpha}\delta a_1 \tag{17}$$

$$\frac{d\delta a_3}{dt} = -3ga^2\sqrt{\alpha}\delta a_3 - 6g\bar{\phi}a\sqrt{\alpha}\delta b_4 \tag{18}$$

$$\frac{d\delta a_7}{dt} = -3ga^2\sqrt{\alpha}\delta a_7 - 6g\bar{\phi}a\sqrt{\alpha}\delta a_{12} \tag{19}$$

$$\frac{d\delta a_{12}}{dt} = -6g\bar{\phi}a\sqrt{\alpha}\delta a_7 - 3ga^2\sqrt{\alpha}\delta a_{12} \tag{20}$$

$$\frac{d\delta a_i}{dt} = -3ga^2\sqrt{\alpha}\delta a_i \ (i = 2, 4, 5, 6, 8, 9, 10, 11) \tag{21}$$

$$\frac{d\delta b_2}{dt} = \left(-4ga^2\sqrt{\alpha} - \frac{1}{9}\alpha\right)\delta b_2 - 4ga^2\sqrt{\alpha}\delta b_5 \tag{22}$$

$$\frac{d\delta b_4}{dt} = -8g\bar{\phi}a\sqrt{\alpha}\delta a_3 + \left(-4ga^2\sqrt{\alpha} - \frac{1}{9}\alpha\right)\delta b_4 \tag{23}$$

$$\frac{d\delta b_5}{dt} = -4ga^2\sqrt{\alpha}\delta b_2 + \left(-4ga^2\sqrt{\alpha} - \frac{1}{9}\alpha\right)\delta b_5 \tag{24}$$

$$\frac{d\delta b_j}{dt} = \left(-4ga^2\sqrt{\alpha} - \frac{1}{9}\alpha\right)\delta b_j \ (j = 1, 3, 6) \tag{25}$$

$$\frac{d\delta c_7}{dt} = -3ga^2\sqrt{\alpha}\delta c_7 - 6g\bar{\phi}a\sqrt{\alpha}\delta c_{12} \tag{26}$$

$$\frac{d\delta c_{12}}{dt} = -6g\bar{\phi}a\sqrt{\alpha}\delta c_7 - 3ga^2\sqrt{\alpha}\delta c_{12} \tag{27}$$

$$\frac{d\delta c_k}{dt} = -3ga^2\sqrt{\alpha}\delta c_k \ (k = 1, 2, 3, 4, 5, 6, 8, 9, 10, 11) \tag{28}$$

$$\frac{d\delta P}{dt} = -h\frac{9a^2}{8\sqrt{\alpha}}\delta P \tag{29}$$

First, it is readily shown that eqs 17, 21, 25, 28, and 29 are decoupled with each other, and hence the set of the equilibrium solutions $a_1 = a$, $a_i = 0$ ($i = 2$, 4, 5, 6, 8, 9, 10, 11), $b_j = 0$ ($j = 1$, 3, 6), $c_k = 0$ ($k = 1$, 2, 3, 4, 5, 6, 8, 9, 10, 11), and $P^2 = 4\sqrt{\alpha}/3$ is linearly stable since g, h, α, and a^2 are positive. Second, we note that eqs 22 and 24 are closed within themselves. The eigenvalues are given by

$$\lambda = -8ga^2\sqrt{\alpha} - \frac{1}{9}\alpha, -\frac{1}{9}\alpha \tag{30}$$

Since these eigenvalues are negative, the solutions $b_2 = b_5 = 0$ are linearly stable. The structure of eqs 26 and 27 is the same as that of eqs 19 and 20. Therefore, we consider only the latter. These two modes δa_7 and δa_{12} give us the stability for the hexagonal disturbance.

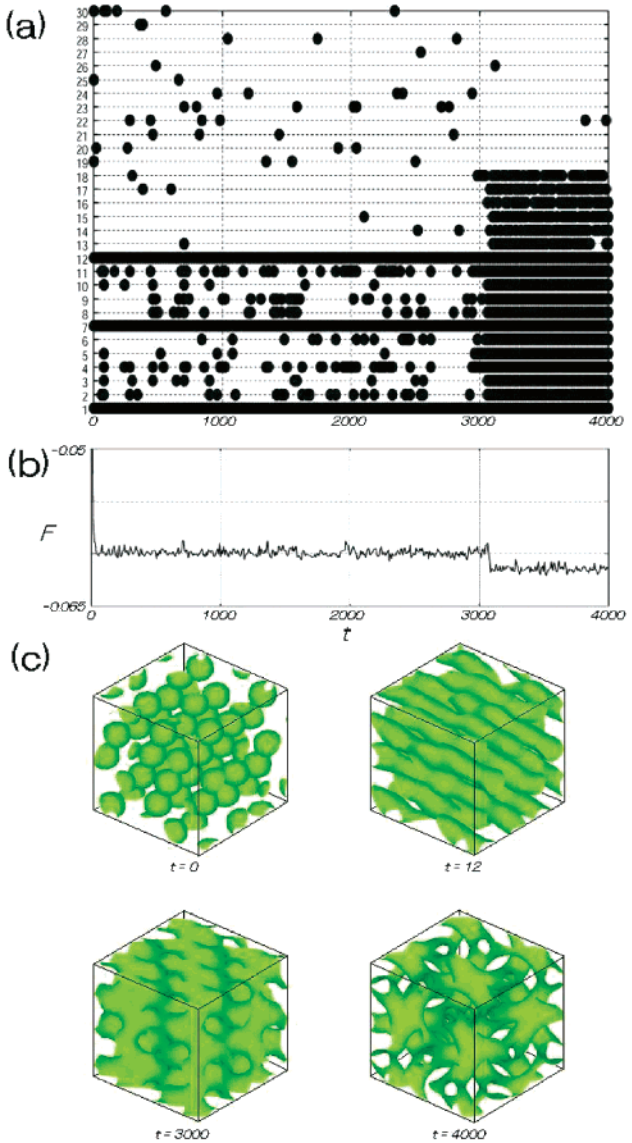

Figure 14. Structural evolution from a BCC for $\bar{\phi} = -0.16$ and $\tau = 2.07$ to a gyroid structure for $\bar{\phi} = -0.16$ and $\tau = 2.5$. (a) Time evolution of the amplitudes. The numbers (1, ..., 30) of the vertical axis correspond to a_1, ..., a_{12}, b_1, ..., b_6, and c_1, ..., c_{12}, respectively. The thick black lines indicate that the absolute value of the amplitudes is larger than 0.035. (b) Time evolution of the free energy. (c) Morphological evolution in the isosurface representation with $\phi_{ISO} = -0.05$.

The stability limit is given by the condition

$$a = 2|\bar{\phi}| \tag{31}$$

This is depicted by the dotted line in Figure 15. The remaining equations (18) and (23) give rise to another instability related to the *Fddd* structure. The condition is given by

$$4ga^2 + \frac{1}{9}\sqrt{\alpha} - 16g\bar{\phi}^2 = 0 \tag{32}$$

The result is indicated by the dashed line in Figure 15.

Comparing with these two stability limits, one notes that a lamellar structure is destabilized by the hexagonal modes earlier than by the *Fddd* modes when τ is decreased. This is consistent with the simulations that LAM → G transition occurs via a hexagonal structure

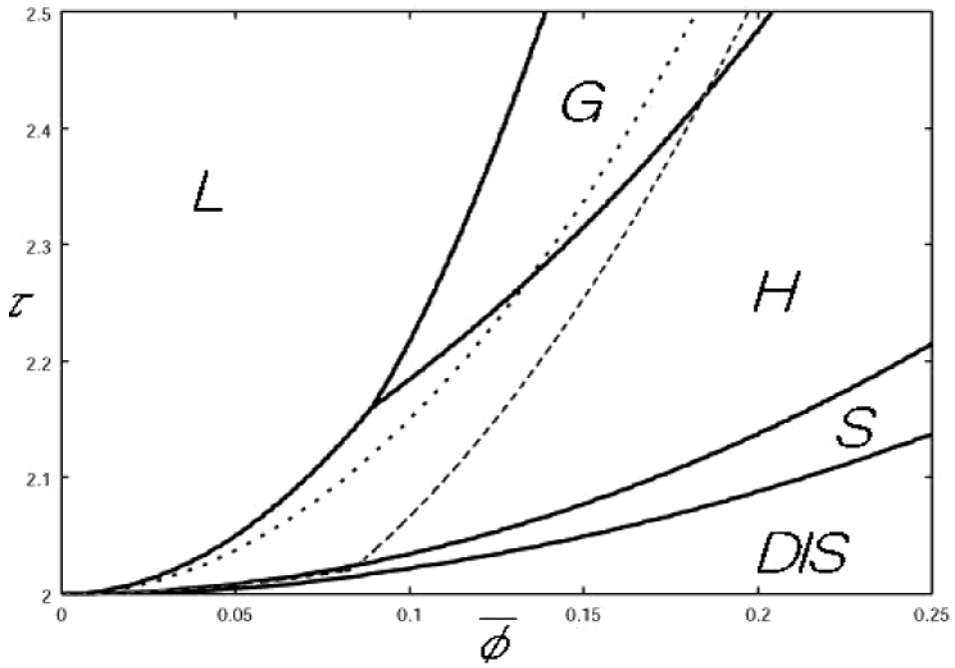

Figure 15. Stability of a lamellar structure. The thick solid curves indicate the same phase boundaries as in Figure 1. The dotted lines is the stability limit for the hexagonal modes whereas the dashed line is the one for the *Fddd* modes.

although the hexagonal phase exists for smaller values of τ than the gyroid phase in the phase diagram.

8. Discussion

We have studied the morphological transitions between microphase-separated states in diblock copolymer melts starting with the suitable free energy functional for microphase separation. The mode expansion method valid in the weak segregation regime has been extended to take account of a gyroid structure. By solving the set of amplitude equations, both order−disorder transitions and order−order transitions have been investigated. Our main findings are summarized as follows:

(1) The equilibrium phase diagram obtained is consistent with the previous results.

(2) In the ordering process from the high-temperature disorder state to the hexagonal phase, we often observe the BCC structure in the evolution of microphase-separated domains. This is not always observed but appears when the parameters for the final hexagonal phase is close to the phase boundary between hexagonal and BCC phases.

(3) In the order−order transitions, the *Fddd* structure appears. We have verified numerically that the *Fddd* structure is a linearly stable equilibrium solution of the amplitude equations, but its free energy is higher than the four fundamental microphase-separated structures. This fact confirms that the *Fddd* structure is metastable. It is noted that the *Fddd* structure is rather persistent which appears in all OOTs except for G → HEX and G → BCC.

(4) In the evolution of a lamellar structure from the disorder state, a perforated lamellar structure is observed (not always but occasionally). This structure is not a stable solution of the amplitude equations and hence just a transient structure. Although not shown, a perforated lamellar structure has also been observed in some simulations of the transitions LAM ↔ BCC and LAM → HEX.

(5) The linear stability analysis of a lamellar solution indicates that this is destabilized dominantly by the hexagonal disturbance among other possible ones.

It is emphasized that (2) and (3) are new theoretical results not reported previously. We note that there are related experiments. Hashimoto et al.[30] have reported that the BCC structure appears in the course of the transition from disorder to hexagonal phases in the experiments of polystyrene-*block*-polyisoprene-*block*-polystylene triblock copolymers. Bates and co-workers[53] have found an unusual equilibrium structure in the experiments of isoprene-*b*-styrene-*b*-ethylene oxide triblock copolymers and have tentatively identified it with the *Fddd* structure. Although these are experiments of triblock copolymers, and are not directly compared with the present results for diblock copolymers, these experimental results are quite encouraging.

Apart from the transitions that involve a gyroid structure, the present theory indicates that the one-mode results of Qi and Wang[43] are essentially unaltered although they have imposed some extra restrictions to the amplitudes. As in ref 43, we have also obtained an unstable perforated lamellar structure. It is possible that this is a saddle point solution of the amplitude equations. However, to confirm this mathematically, one needs to determine the precise values of the amplitudes at the saddle point. Since this is difficult technically, we do not go into this problem here.

We make some remarks about the approximations employed in the present paper. We have ignored the space dependence and the phase degree of freedom of the amplitudes. Therefore, nucleation and growth of new domains in OOTs are not studied. Local distortion of the equilibrium structures is also not described. The space dependence of the amplitudes is expected to be necessary even in disorder−order transitions since some long wavelength modes may influence the kinetics.[54,55] We have introduced phenomenologically the time evolution equation for the spatial period. This is related to the ignore of the phase variables. These approximations

are indeed crude for kinetics of morphological transitions. However, since there are 30 amplitudes, if these are considered fully, the theory would be too complicated and useless to explore possible intermediate or transient structures and to see the details of reconnection of domains during the transitions as have been achieved in the present paper.

In our opinion, the mode expansion method generalized to the nonuniform amplitudes and phases should be formulated in such a way that it is more suitable for analytical theory. For example, structure and motion of a planar grain boundary between lamellar and gyroid structures influenced by the elastic misfit due to the difference of the periods are an interesting fundamental problem relevant to the kinetics of morphological transitions. In this case, the number of the independent amplitudes and phases is reduced by symmetry, and one may develop an analytically tractable approach. It is our expectation that the present theory of the nontrivial zeroth-order approximation would provide a basis for such development.

Acknowledgment. We thank M. Imai, T. Kawakatsu, A. Saeki, and T. Teramoto for valuable discussions. This work was supported by the Grant-in-Aid of Ministry of Education, Science and Culture of Japan.

Appendix A

Equations for the amplitudes a_i ($i = 1, ..., 12$), b_j ($j = 1, ..., 6$), and c_k ($k = 1, ..., 12$) are given by

$$\frac{da_1}{dt} = A_1 a_1 - 6gQ^2(\bar{\phi} a_3 b_4 + \bar{\phi} a_7 a_{12} + \bar{\phi} c_7 c_{12} + a_1 b_2 b_5 + a_2 a_3 a_4 + a_2 a_5 a_8 + a_2 a_6 a_7 + a_3 b_1 b_2 + a_3 b_1 b_5 + a_3 b_2 b_6 + a_3 b_5 b_6 + a_4 a_9 a_{10} + a_4 a_{11} a_{12} + a_5 a_{10} b_2 + a_5 a_{10} b_5 + a_5 a_{12} b_6 + a_6 a_9 b_3 + a_6 a_9 b_6 + a_6 a_{11} b_2 + a_6 a_{11} b_4 + a_6 a_{11} b_5 + a_7 a_{10} b_1 + a_7 c_1 c_7 + a_8 a_9 b_4 + a_8 a_{11} b_1 + a_8 a_{11} b_3 + a_{12} c_1 c_{12} + b_4 c_8 c_9)$$

$$\frac{da_2}{dt} = A_2 a_2 - 6gQ^2(\bar{\phi} a_4 b_3 + \bar{\phi} a_6 a_{10} + \bar{\phi} c_2 c_{10} + a_1 a_3 a_4 + a_1 a_5 a_8 + a_1 a_6 a_7 + a_2 b_2 b_6 + a_3 a_9 a_{10} + a_3 a_{11} a_{12} + a_4 b_1 b_2 + a_4 b_1 b_6 + a_4 b_2 b_5 + a_4 b_5 b_6 + a_5 a_9 b_1 + a_5 a_9 b_4 + a_5 a_{11} b_3 + a_6 a_{12} b_1 + a_6 c_6 c_{10} + a_7 a_9 b_2 + a_7 a_9 b_3 + a_7 a_9 b_6 + a_7 a_{11} b_4 + a_7 a_{11} b_5 + a_8 a_{10} b_5 + a_8 a_{12} b_2 + a_8 a_{12} b_6 + a_{10} c_2 c_6 + b_3 c_4 c_{11})$$

$$\frac{da_3}{dt} = A_3 a_3 - 6gQ^2(\bar{\phi} a_1 b_4 + \bar{\phi} a_8 a_9 + \bar{\phi} c_8 c_9 + a_1 a_2 a_4 + a_1 b_1 b_2 + a_1 b_1 b_5 + a_1 b_2 b_6 + a_1 b_5 b_6 + a_2 a_9 a_{10} + a_2 a_{11} a_{12} + a_3 b_1 b_6 + a_4 a_5 a_8 + a_4 a_6 a_7 + a_5 a_{10} b_1 + a_5 a_{10} b_4 + a_5 a_{10} b_6 + a_5 a_{12} b_3 + a_5 a_{12} b_5 + a_6 a_9 b_5 + a_6 a_{11} b_1 + a_6 a_{11} b_6 + a_7 a_{10} b_2 + a_7 a_{10} b_3 + a_7 a_{12} b_4 + a_8 a_{11} b_2 + a_8 c_3 c_8 + a_9 c_3 c_9 + b_4 c_7 c_{12})$$

$$\frac{da_4}{dt} = A_4 a_4 - 6gQ^2(\bar{\phi} a_2 b_3 + \bar{\phi} a_5 a_{11} + \bar{\phi} c_4 c_{11} + a_1 a_2 a_3 + a_1 a_9 a_{10} + a_1 a_{11} a_{12} + a_2 b_1 b_2 + a_2 b_1 b_6 + a_2 b_2 b_5 + a_2 b_5 b_6 + a_3 a_5 a_8 + a_3 a_6 a_7 + a_4 b_1 b_5 + a_5 a_9 b_2 + a_5 c_4 c_5 + a_6 a_{10} b_3 + a_6 a_{12} b_2 + a_6 a_{12} b_4 + a_7 a_9 b_1 + a_7 a_9 b_5 + a_7 a_{11} b_6 + a_8 a_{10} b_4 + a_8 a_{10} b_6 + a_8 a_{12} b_1 + a_8 a_{12} b_3 + a_8 a_{12} b_5 + a_{11} c_5 c_{11} + b_3 c_2 c_{10})$$

$$\frac{da_5}{dt} = A_5 a_5 - 6gQ^2(\bar{\phi} a_4 a_{11} + \bar{\phi} a_7 b_6 + \bar{\phi} c_5 c_{11} + a_1 a_2 a_8 + a_1 a_{10} b_2 + a_1 a_{10} b_5 + a_1 a_{12} b_6 + a_2 a_9 b_1 + a_2 a_9 b_4 + a_2 a_{11} b_3 + a_3 a_4 a_8 + a_3 a_{10} b_1 + a_3 a_{10} b_4 + a_3 a_{10} b_6 + a_3 a_{12} b_3 + a_3 a_{12} b_5 + a_4 a_9 b_2 + a_4 c_4 c_5 + a_5 b_1 b_4 + a_6 a_7 a_8 + a_6 a_9 a_{12} + a_6 a_{10} a_{11} + a_7 b_1 b_2 + a_7 b_1 b_3 + a_7 b_2 b_4 + a_7 b_3 b_4 + a_{11} c_4 c_{11} + b_6 c_1 c_{12})$$

$$\frac{da_6}{dt} = A_6 a_6 - 6gQ^2(\bar{\phi} a_2 a_{10} + \bar{\phi} a_8 b_5 + \bar{\phi} c_2 c_6 + a_1 a_2 a_7 + a_1 a_9 b_3 + a_1 a_9 b_6 + a_1 a_{11} b_2 + a_1 a_{11} b_4 + a_1 a_{11} b_5 + a_2 a_{12} b_1 + a_2 c_6 c_{10} + a_3 a_4 a_7 + a_3 a_9 b_5 + a_3 a_{11} b_1 + a_3 a_{11} b_6 + a_4 a_{10} b_3 + a_4 a_{12} b_2 + a_4 a_{12} b_4 + a_5 a_7 a_8 + a_5 a_9 a_{12} + a_5 a_{10} a_{11} + a_6 b_2 b_4 + a_8 b_1 b_2 + a_8 b_1 b_4 + a_8 b_2 b_3 + a_8 b_3 b_4 + a_{10} c_2 c_{10} + b_5 c_3 c_9)$$

$$\frac{da_7}{dt} = A_7 a_7 - 6gQ^2(\bar{\phi} a_1 a_{12} + \bar{\phi} a_5 b_6 + \bar{\phi} c_1 c_{12} + a_1 a_2 a_6 + a_1 a_{10} b_1 + a_1 c_1 c_7 + a_2 a_9 b_2 + a_2 a_9 b_3 + a_2 a_9 b_6 + a_2 a_{11} b_4 + a_2 a_{11} b_5 + a_3 a_4 a_6 + a_3 a_{10} b_2 + a_3 a_{10} b_3 + a_3 a_{12} b_4 + a_4 a_9 b_1 + a_4 a_9 b_5 + a_4 a_{11} b_6 + a_5 a_6 a_8 + a_5 b_1 b_2 + a_5 b_1 b_3 + a_5 b_2 b_4 + a_5 b_3 b_4 + a_7 b_2 b_3 + a_8 a_9 a_{12} + a_8 a_{10} a_{11} + a_{12} c_7 c_{12} + b_6 c_5 c_{11})$$

$$\frac{da_8}{dt} = A_8 a_8 - 6gQ^2(\bar{\phi} a_3 a_9 + \bar{\phi} a_6 b_5 + \bar{\phi} c_3 c_9 + a_1 a_2 a_5 + a_1 a_9 b_4 + a_1 a_{11} b_1 + a_1 a_{11} b_3 + a_2 a_{10} b_5 + a_2 a_{12} b_2 + a_2 a_{12} b_6 + a_3 a_4 a_5 + a_3 a_{11} b_2 + a_3 c_3 c_8 + a_4 a_{10} b_4 + a_4 a_{10} b_6 + a_4 a_{12} b_1 + a_4 a_{12} b_3 + a_4 a_{12} b_5 + a_5 a_6 a_7 + a_6 b_1 b_2 + a_6 b_1 b_4 + a_6 b_2 b_3 + a_6 b_3 b_4 + a_7 a_9 a_{12} + a_7 a_{10} a_{11} + a_8 b_1 b_3 + a_9 c_8 c_9 + b_5 c_2 c_6)$$

$$\frac{da_9}{dt} = A_9 a_9 - 6gQ^2(\bar{\phi} a_3 a_8 + \bar{\phi} a_{11} b_2 + \bar{\phi} c_3 c_8 + a_1 a_4 a_{10} + a_1 a_6 b_3 + a_1 a_6 b_6 + a_1 a_8 b_4 + a_2 a_3 a_{10} + a_2 a_5 b_1 + a_2 a_5 b_4 + a_2 a_7 b_2 + a_2 a_7 b_3 + a_2 a_7 b_6 + a_3 a_6 b_5 + a_3 c_3 c_9 + a_4 a_5 b_2 + a_4 a_7 b_1 + a_4 a_7 b_5 + a_5 a_6 a_{12} + a_7 a_8 a_{12} + a_8 c_8 c_9 + a_9 b_3 b_6 + a_{10} a_{11} a_{12} + a_{11} b_3 b_4 + a_{11} b_3 b_5 + a_{11} b_4 b_6 + a_{11} b_5 b_6 + b_2 c_4 c_5)$$

$$\frac{da_{10}}{dt} = A_{10} a_{10} - 6gQ^2(\bar{\phi} a_2 a_6 + \bar{\phi} a_{12} b_1 + \bar{\phi} c_6 c_{10} + a_1 a_4 a_9 + a_1 a_5 b_2 + a_1 a_5 b_5 + a_1 a_7 b_1 + a_2 a_3 a_9 + a_2 a_8 b_5 + a_2 c_2 c_6 + a_3 a_5 b_1 + a_3 a_5 b_4 + a_3 a_5 b_6 + a_3 a_7 b_2 + a_3 a_7 b_3 + a_4 a_6 b_3 + a_4 a_8 b_4 + a_4 a_8 b_6 + a_5 a_6 a_{11} + a_6 c_2 c_{10} + a_7 a_8 a_{11} + a_9 a_{11} a_{12} + a_{10} b_4 b_6 + a_{12} b_3 b_4 + a_{12} b_3 b_6 + a_{12} b_4 b_5 + a_{12} b_5 b_6 + b_1 c_1 c_7)$$

$$\frac{da_{11}}{dt} = A_{11} a_{11} - 6gQ^2(\bar{\phi} a_4 a_5 + \bar{\phi} a_9 b_2 + \bar{\phi} c_4 c_5 + a_1 a_4 a_{12} + a_1 a_6 b_2 + a_1 a_6 b_4 + a_1 a_6 b_5 + a_1 a_8 b_1 + a_1 a_8 b_3 + a_2 a_3 a_{12} + a_2 a_5 b_3 + a_2 a_7 b_4 + a_2 a_7 b_5 + a_3 a_6 b_1 + a_3 a_6 b_6 + a_3 a_8 b_2 + a_4 a_7 b_6 + a_4 c_5 c_{11} + a_5 a_6 a_{10} + a_5 c_4 c_{11} + a_7 a_8 a_{10} + a_9 a_{10} a_{12} + a_9 b_3 b_4 + a_9 b_3 b_5 + a_9 b_4 b_6 + a_9 b_5 b_6 + a_{11} b_4 b_5 + b_2 c_3 c_8)$$

$$\frac{da_{12}}{dt} = A_{12}a_{12} - 6gQ^2(\bar{\phi}a_1a_7 + \bar{\phi}a_{10}b_1 + \bar{\phi}c_1c_7 + a_1a_4a_{11} + a_1a_5b_6 + a_1c_1c_{12} + a_2a_3a_{11} + a_2a_6b_1 + a_2a_8b_2 + a_2a_8b_6 + a_3a_5b_3 + a_3a_5b_5 + a_3a_7b_4 + a_4a_6b_2 + a_4a_6b_4 + a_4a_8b_1 + a_4a_8b_3 + a_4a_8b_5 + a_5a_6a_9 + a_7a_8a_9 + a_7c_7c_{12} + a_9a_{10}a_{11} + a_{10}b_3b_4 + a_{10}b_3b_6 + a_{10}b_4b_5 + a_{10}b_5b_6 + a_{12}b_3b_5 + b_1c_6c_{10})$$

$$\frac{db_1}{dt} = B_1b_1 - 6gP^2(\bar{\phi}a_{10}a_{12} + \bar{\phi}b_3b_6 + \bar{\phi}b_4b_5 + a_1a_3b_2 + a_1a_3b_5 + a_1a_7a_{10} + a_1a_8a_{11} + a_2a_4b_2 + a_2a_4b_6 + a_2a_5a_9 + a_2a_6a_{12} + a_3a_5a_{10} + a_3a_6a_{11} + a_4a_7a_9 + a_4a_8a_{12} + a_5a_7b_2 + a_5a_7b_3 + a_6a_8b_2 + a_6a_8b_4 + a_{10}c_1c_7 + a_{12}c_6c_{10} + b_2b_3b_4 + b_2b_5b_6) - 3gP^2({a_3}^2b_6 + {a_4}^2b_5 + {a_5}^2b_4 + {a_8}^2b_3)$$

$$\frac{db_2}{dt} = B_2b_2 - 6gP^2(\bar{\phi}a_9a_{11} + \bar{\phi}b_3b_5 + \bar{\phi}b_4b_6 + a_1a_3b_1 + a_1a_3b_6 + a_1a_5a_{10} + a_1a_6a_{11} + a_2a_4b_1 + a_2a_4b_5 + a_2a_7a_9 + a_2a_8a_{12} + a_3a_7a_{10} + a_3a_8a_{11} + a_4a_5a_9 + a_4a_6a_{12} + a_5a_7b_1 + a_5a_7b_4 + a_6a_8b_1 + a_6a_8b_3 + a_9c_4c_5 + a_{11}c_3c_8 + b_1b_3b_4 + b_1b_5b_6) - 3gP^2({a_1}^2b_5 + {a_2}^2b_6 + {a_6}^2b_4 + {a_7}^2b_3)$$

$$\frac{db_3}{dt} = B_3b_3 - 6gP^2(\bar{\phi}a_2a_4 + \bar{\phi}b_1b_6 + \bar{\phi}b_2b_5 + a_1a_6a_9 + a_1a_8a_{11} + a_2a_5a_{11} + a_2a_7a_9 + a_2c_4c_{11} + a_3a_5a_{12} + a_3a_7a_{10} + a_4a_6a_{10} + a_4a_8a_{12} + a_4c_2c_{10} + a_5a_7b_1 + a_5a_7b_4 + a_6a_8b_2 + a_6a_8b_4 + a_9a_{11}b_4 + a_9a_{11}b_5 + a_{10}a_{12}b_4 + a_{10}a_{12}b_6 + b_1b_2b_4 + b_4b_5b_6) - 3gP^2({a_7}^2b_2 + {a_8}^2b_1 + {a_9}^2b_6 + {a_{12}}^2b_5)$$

$$\frac{db_4}{dt} = B_4b_4 - 6gP^2(\bar{\phi}a_1a_3 + \bar{\phi}b_1b_5 + \bar{\phi}b_2b_6 + a_1a_6a_{11} + a_1a_8a_9 + a_1c_8c_9 + a_2a_5a_9 + a_2a_7a_{11} + a_3a_5a_{10} + a_3a_7a_{12} + a_3c_7c_{12} + a_4a_6a_{12} + a_4a_8a_{10} + a_5a_7b_2 + a_5a_7b_3 + a_6a_8b_1 + a_6a_8b_3 + a_9a_{11}b_3 + a_9a_{11}b_6 + a_{10}a_{12}b_3 + a_{10}a_{12}b_5 + b_1b_2b_3 + b_3b_5b_6) - 3gP^2({a_5}^2b_1 + {a_6}^2b_2 + {a_{10}}^2b_6 + {a_{11}}^2b_5)$$

$$\frac{db_5}{dt} = B_5b_5 - 6gP^2(\bar{\phi}a_6a_8 + \bar{\phi}b_1b_4 + \bar{\phi}b_2b_3 + a_1a_3b_1 + a_1a_3b_6 + a_1a_5a_{10} + a_1a_6a_{11} + a_2a_4b_2 + a_2a_4b_6 + a_2a_7a_{11} + a_2a_8a_{10} + a_3a_5a_{12} + a_3a_6a_9 + a_4a_7a_9 + a_4a_8a_{12} + a_6c_3c_9 + a_8c_2c_6 + a_9a_{11}b_3 + a_9a_{11}b_6 + a_{10}a_{12}b_4 + a_{10}a_{12}b_6 + b_1b_2b_6 + b_3b_4b_6) - 3gP^2({a_1}^2b_2 + {a_4}^2b_1 + {a_{11}}^2b_4 + {a_{12}}^2b_3)$$

$$\frac{db_6}{dt} = B_6b_6 - 6gP^2(\bar{\phi}a_5a_7 + \bar{\phi}b_1b_3 + \bar{\phi}b_2b_4 + a_1a_3b_2 + a_1a_3b_5 + a_1a_5a_{12} + a_1a_6a_9 + a_2a_4b_1 + a_2a_4b_5 + a_2a_7a_9 + a_2a_8a_{12} + a_3a_5a_{10} + a_3a_6a_{11} + a_4a_7a_{11} + a_4a_8a_{10} + a_5c_1c_{12} + a_7c_5c_{11} + a_9a_{11}b_4 + a_9a_{11}b_5 + a_{10}a_{12}b_3 + a_{10}a_{12}b_5 + b_1b_2b_5 + b_3b_4b_5) - 3gP^2({a_2}^2b_2 + {a_3}^2b_1 + {a_9}^2b_3 + {a_{10}}^2b_4)$$

$$\frac{dc_1}{dt} = C_1c_1 - 6gQ^2(\bar{\phi}a_7c_{12} + \bar{\phi}a_{12}c_7 + a_1a_7c_7 + a_1a_{12}c_{12} + a_5b_6c_{12} + a_{10}b_1c_7 + c_4c_6c_8)$$

$$\frac{dc_2}{dt} = C_2c_2 - 6gQ^2(\bar{\phi}a_2c_{10} + \bar{\phi}a_6c_6 + a_2a_{10}c_6 + a_4b_3c_{10} + a_6a_{10}c_{10} + a_8b_5c_6 + c_9c_{11}c_{12})$$

$$\frac{dc_3}{dt} = C_3c_3 - 6gQ^2(\bar{\phi}a_8c_9 + \bar{\phi}a_9c_8 + a_3a_8c_8 + a_3a_9c_9 + a_6b_5c_9 + a_{11}b_2c_8 + c_5c_7c_{10})$$

$$\frac{dc_4}{dt} = C_4c_4 - 6gQ^2(\bar{\phi}a_4c_{11} + \bar{\phi}a_{11}c_5 + a_2b_3c_{11} + a_4a_5c_5 + a_5a_{11}c_{11} + a_9b_2c_5 + c_1c_6c_8)$$

$$\frac{dc_5}{dt} = C_5c_5 - 6gQ^2(\bar{\phi}a_5c_{11} + \bar{\phi}a_{11}c_4 + a_4a_5c_4 + a_4a_{11}c_{11} + a_7b_6c_{11} + a_9b_2c_4 + c_3c_7c_{10})$$

$$\frac{dc_6}{dt} = C_6c_6 - 6gQ^2(\bar{\phi}a_6c_2 + \bar{\phi}a_{10}c_{10} + a_2a_6c_{10} + a_2a_{10}c_2 + a_8b_5c_2 + a_{12}b_1c_{10} + c_1c_4c_8)$$

$$\frac{dc_7}{dt} = C_7c_7 - 6gQ^2(\bar{\phi}a_1c_{12} + \bar{\phi}a_{12}c_1 + a_1a_7c_1 + a_3b_4c_{12} + a_7a_{12}c_{12} + a_{10}b_1c_1 + c_3c_5c_{10})$$

$$\frac{dc_8}{dt} = C_8c_8 - 6gQ^2(\bar{\phi}a_3c_9 + \bar{\phi}a_9c_3 + a_1b_4c_9 + a_3a_8c_3 + a_8a_9c_9 + a_{11}b_2c_3 + c_1c_4c_6)$$

$$\frac{dc_9}{dt} = C_9c_9 - 6gQ^2(\bar{\phi}a_3c_8 + \bar{\phi}a_8c_3 + a_1b_4c_8 + a_3a_9c_3 + a_6b_5c_3 + a_8a_9c_8 + c_2c_{11}c_{12})$$

$$\frac{dc_{10}}{dt} = C_{10}c_{10} - 6gQ^2(\bar{\phi}a_2c_2 + \bar{\phi}a_{10}c_6 + a_2a_6c_6 + a_4b_3c_2 + a_6a_{10}c_2 + a_{12}b_1c_6 + c_3c_5c_7)$$

$$\frac{dc_{11}}{dt} = C_{11}c_{11} - 6gQ^2(\bar{\phi}a_4c_4 + \bar{\phi}a_5c_5 + a_2b_3c_4 + a_4a_{11}c_5 + a_5a_{11}c_4 + a_7b_6c_5 + c_2c_9c_{12})$$

$$\frac{dc_{12}}{dt} = C_{12}c_{12} - 6gQ^2(\bar{\phi}a_1c_7 + \bar{\phi}a_7c_1 + a_1a_{12}c_1 + a_3b_4c_7 + a_5b_6c_1 + a_7a_{12}c_7 + c_2c_9c_{11}) \quad (33)$$

The coefficients A_i, B_j, and C_k are defined by

$$A_i = (-Q^4 + \tau Q^2 - \alpha) - gQ^2[3(\bar{\phi}^2 - {a_i}^2) + 6(\sum_{l=1}^{12}{a_l}^2 + \sum_{m=1}^{6}{b_m}^2 + \sum_{n=1}^{12}{c_n}^2)]$$

$$B_j = (-P^4 + \tau P^2 - \alpha) - gP^2[3(\bar{\phi}^2 - {b_j}^2) + 6(\sum_{l=1}^{12}{a_l}^2 + \sum_{m=1}^{6}{b_m}^2 + \sum_{n=1}^{12}{c_n}^2)]$$

$$C_k = (-Q^4 + \tau Q^2 - \alpha) - gQ^2[3(\bar{\phi}^2 - {c_k}^2) + 6(\sum_{l=1}^{12} {a_l}^2 + \sum_{m=1}^{6} {b_m}^2 + \sum_{n=1}^{12} {c_n}^2)] \quad (34)$$

Appendix B

The free energy in terms of the amplitudes and the period P is given by

$$F_{amp} = F_{DIS} + \left(\frac{3}{4}P^2 + \frac{4\alpha}{3P^2} - \tau + 3g\bar{\phi}^2\right)(\sum_{i=1}^{12} {a_i}^2 + \sum_{k=1}^{12} {c_k}^2) + \left(P^2 + \frac{\alpha}{P^2} - \tau + 3g\bar{\phi}^2\right)\sum_{j=1}^{6} {b_j}^2 + (g/4)[12(\sum_{i=1}^{12} {a_i}^2 + \sum_{j=1}^{6} {b_j}^2 + \sum_{k=1}^{12} {c_k}^2)^2 - 6(\sum_{i=1}^{12} {a_i}^4 + \sum_{j=1}^{6} {b_j}^4 + \sum_{k=1}^{12} {c_k}^4) + 24({a_1}^2 b_2 b_5 + {a_2}^2 b_2 b_6 + {a_3}^2 b_1 b_6 + {a_4}^2 b_1 b_5 + {a_5}^2 b_1 b_4 + {a_6}^2 b_2 b_4 + {a_7}^2 b_2 b_3 + {a_8}^2 b_1 b_3 + {a_9}^2 b_3 b_6 + {a_{10}}^2 b_4 b_6 + {a_{11}}^2 b_4 b_5 + {a_{12}}^2 b_3 b_5) + 48\bar{\phi}(a_1 a_3 b_4 + a_1 a_7 a_{12} + a_1 c_7 c_{12} + a_2 a_4 b_3 + a_2 a_6 a_{10} + a_2 c_2 c_{10} + a_3 a_8 a_9 + a_3 c_8 c_9 + a_4 a_5 a_{11} + a_4 c_4 c_{11} + a_5 a_7 b_6 + a_5 c_5 c_{11} + a_6 a_8 b_5 + a_6 c_2 c_6 + a_7 c_1 c_{12} + a_8 c_3 c_9 + a_9 a_{11} b_2 + a_9 c_3 c_8 + a_{10} a_{12} b_1 + a_{10} c_6 c_{10} + a_{11} c_4 c_5 + a_{12} c_1 c_7 + b_1 b_3 b_6 + b_1 b_4 b_5 + b_2 b_3 b_5 + b_2 b_4 b_6) + 48(a_1 a_2 a_3 a_4 + a_1 a_2 a_5 a_8 + a_1 a_2 a_6 a_7 + a_1 a_3 b_1 b_2 + a_1 a_3 b_1 b_5 + a_1 a_3 b_2 b_6 + a_1 a_3 b_5 b_6 + a_1 a_4 a_9 a_{10} + a_1 a_4 a_{11} a_{12} + a_1 a_5 a_{10} b_2 + a_1 a_5 a_{10} b_5 + a_1 a_5 a_{12} b_6 + a_1 a_6 a_9 b_3 + a_1 a_6 a_9 b_6 + a_1 a_6 a_{11} b_2 + a_1 a_6 a_{11} b_4 + a_1 a_6 a_{11} b_5 + a_1 a_7 a_{10} b_1 + a_1 a_7 c_1 c_7 + a_1 a_8 a_9 b_4 + a_1 a_8 a_{11} b_1 + a_1 a_8 a_{11} b_3 + a_1 a_{12} c_1 c_{12} + a_1 b_4 c_8 c_9 + a_2 a_3 a_9 a_{10} + a_2 a_3 a_{11} a_{12} + a_2 a_4 b_1 b_2 + a_2 a_4 b_1 b_6 + a_2 a_4 b_2 b_5 + a_2 a_4 b_5 b_6 + a_2 a_5 a_9 b_1 + a_2 a_5 a_9 b_4 + a_2 a_5 a_{11} b_3 + a_2 a_6 a_{12} b_1 + a_2 a_6 c_6 c_{10} + a_2 a_7 a_9 b_2 + a_2 a_7 a_9 b_3 + a_2 a_7 a_9 b_6 + a_2 a_7 a_{11} b_4 + a_2 a_7 a_{11} b_5 + a_2 a_8 a_{10} b_5 + a_2 a_8 a_{12} b_2 + a_2 a_8 a_{12} b_6 + a_2 a_{10} c_2 c_6 + a_2 b_3 c_4 c_{11} + a_3 a_4 a_5 a_8 + a_3 a_4 a_6 a_7 + a_3 a_5 a_{10} b_1 + a_3 a_5 a_{10} b_4 + a_3 a_5 a_{10} b_6 + a_3 a_5 a_{12} b_3 + a_3 a_5 a_{12} b_5 + a_3 a_6 a_9 b_5 + a_3 a_6 a_{11} b_1 + a_3 a_6 a_{11} b_6 + a_3 a_7 a_{10} b_2 + a_3 a_7 a_{10} b_3 + a_3 a_7 a_{12} b_4 + a_3 a_8 a_{11} b_2 + a_3 a_8 c_3 c_8 + a_3 a_9 c_3 c_9 + a_3 b_4 c_7 c_{12} + a_4 a_5 a_9 b_2 + a_4 a_5 c_4 c_5 + a_4 a_6 a_{10} b_3 + a_4 a_6 a_{12} b_2 + a_4 a_6 a_{12} b_4 + a_4 a_7 a_9 b_1 + a_4 a_7 a_9 b_5 + a_4 a_7 a_{11} b_6 + a_4 a_8 a_{10} b_4 + a_4 a_8 a_{10} b_6 + a_4 a_8 a_{12} b_1 + a_4 a_8 a_{12} b_3 + a_4 a_8 a_{12} b_5 + a_4 a_{11} c_5 c_{11} + a_4 b_3 c_2 c_{10} + a_5 a_6 a_7 a_8 + a_5 a_6 a_9 a_{12} + a_5 a_6 a_{10} a_{11} + a_5 a_7 b_1 b_2 + a_5 a_7 b_1 b_3 + a_5 a_7 b_2 b_4 + a_5 a_7 b_3 b_4 + a_5 a_{11} c_4 c_{11} + a_5 b_6 c_1 c_{12} + a_6 a_8 b_1 b_2 + a_6 a_8 b_1 b_4 + a_6 a_8 b_2 b_3 + a_6 a_8 b_3 b_4 + a_6 a_{10} c_2 c_{10} + a_6 b_5 c_3 c_9 + a_7 a_8 a_9 a_{12} + a_7 a_8 a_{10} a_{11} + a_7 a_{12} c_7 c_{12} + a_7 b_6 c_5 c_{11} + a_8 a_9 c_8 c_9 + a_8 b_5 c_2 c_6 + a_9 a_{10} a_{11} a_{12} + a_9 a_{11} b_3 b_4 + a_9 a_{11} b_3 b_5 + a_9 a_{11} b_4 b_6 + a_9 a_{11} b_5 b_6 + a_9 b_2 c_4 c_5 + a_{10} a_{12} b_3 b_4 + a_{10} a_{12} b_3 b_6 + a_{10} a_{12} b_4 b_5 + a_{10} a_{12} b_5 b_6 + a_{10} b_1 c_1 c_7 + a_{11} b_2 c_3 c_8 + a_{12} b_1 c_6 c_{10} + b_1 b_2 b_3 b_4 + b_1 b_2 b_5 b_6 + b_3 b_4 b_5 b_6 + c_1 c_4 c_6 c_8 + c_2 c_9 c_{11} c_{12} + c_3 c_5 c_7 c_{10})] \quad (35)$$

where $F_{DIS} = -\tau\bar{\phi}^2/2 + g\bar{\phi}^4/4$ is the free energy for the disorder state.

The equilibrium free energy for several specific structures is evaluated as follows. Putting $a_i = A_G \neq 0$, $b_j = B_G \neq 0$, and $c_k = 0$, the free energy for gyroid is given by

$$F_G = F_{DIS} + 12\left(\frac{3}{4}P^2 + \frac{4\alpha}{3P^2} - \tau + 3g\right){A_G}^2 + 6\left(P^2 + \frac{\alpha}{P^2} - \tau + 3g\right){B_G}^2 + 3g[102{A_G}^4 + 72{A_G}^2{B_G}^2 + 45{B_G}^4 + 16\bar{\phi}({A_G}^3 + {B_G}^3) - 24\bar{\phi}{A_G}^2 B_G] \quad (36)$$

In the same way, the free energies of lamellar, F_L, hexagonal structure, F_H, and BCC, F_B, are given respectively by

$$F_L = F_{DIS} + \left(P^2 + \frac{\alpha}{P^2} - \tau + 3g\bar{\phi}^2\right){A_L}^2 + \frac{3}{2}g{A_L}^4 \quad (37)$$

$$F_H = F_{DIS} + 3\left(P^2 + \frac{\alpha}{P^2} - \tau + 3g\bar{\phi}^2\right){A_H}^2 + 3g\left(4\bar{\phi}{A_H}^3 + \frac{15}{2}{A_H}^4\right) \quad (38)$$

$$F_B = F_{DIS} + 6\left(P^2 + \frac{\alpha}{P^2} - \tau + 3g\bar{\phi}^2\right){A_B}^2 + 3g(16\bar{\phi}{A_B}^3 + 45{A_B}^4) \quad (39)$$

where A_L, A_H, and A_B are the amplitude for LAM, HEX, and BCC, respectively.

Appendix C

In Tables 1−3, we present 12 stable equilibrium solutions of the amplitude equations except for the *Fddd* and IM solutions described in section 4.

We do not exclude the possibility that there might be other stable solutions. It is a difficult task, however, to search for all such solutions since we have no powerful algorithm to do so at present.

References and Notes

(1) Matsen, M. W.; Schick, M. *Phys. Rev. Lett.* **1994**, *72*, 2660.
(2) Matsen, M. W.; Bates, F. S. *Macromolecules* **1996**, *29*, 7641. Matsen, M. W.; Bates, F. S. *Macromolecules* **1996**, *29*, 1091.
(3) Milner, S. T.; Olmsted, P. D. *J. Phys. II* **1997**, *7*, 249.
(4) Matsen, M. W. *J. Phys.: Condens. Matter* **2002**, *14*, R21.
(5) Foerster, S.; Khandpur, A. K.; Zhao, J.; Bates, F. S.; Hamley, I. W.; Ryan, A. J.; Bras, W. *Macromolecules* **1994**, *27*, 6922.
(6) Khandpur, A. K.; Foerster, S.; Bates, F. S.; Hamley, I. W.; Ryan, A. J.; Bras, W.; Almdal, K.; Mortensen, K. *Macromolecules* **1995**, *28*, 8796.
(7) Zhao, J.; Majumdar, B.; Schulz, M. F.; Bates, F. S.; Almdal, K.; Mortensen, K.; Hajduk, D. A.; Gruner, S. M. *Macromolecules* **1996**, *29*, 1204.
(8) Foudas, G.; Ulrich, R.; Wiesner, U. *J. Chem. Phys.* **1999**, *110*, 652.
(9) Kossuth, M. B.; Morse, D. C.; Bates, F. S. *J. Rheol.* **1999**, *43*, 167.
(10) Hamley, I. W.; Castelletto, V.; Floudas, G.; Schipper, F. *Macromolecules* **2002**, *35*, 8839.
(11) Lodge, T. P.; Hanley, K. J.; Pudil, B.; Alahapperuma, V. *Macromolecules* **2003**, *36*, 816.
(12) Chastek, T. Q.; Lodge, T. P. *Macromolecules* **2003**, *36*, 7672.
(13) Kimishima, K.; Koga, T.; Hashimoto, T. *Macromolecules* **2000**, *33*, 968.
(14) Krishnamoorti, R.; Silva, A. S.; Modi, M. A.; Hammouda, B. *Macromolecules* **2000**, *33*, 3803. Krishnamoorti, R.; Modi, M. A.; Tse, M. F.; Wang, H. C. *Macromolecules* **2000**, *33*, 3810.

(15) Lee, H. H.; Jeong, W. Y.; Kim, K.; Ihn, K. J.; Kornfield, J. A.; Wang, Z. G.; Qi, S. *Macromolecules* **2002**, *35*, 785.
(16) Hajduk, D. A.; Harper, P. E.; Gruner, S. M.; Honeker, C. C.; Kim, G.; Thomas, E. L. *Macromolecules* **1994**, *27*, 4063.
(17) Wang, C. Y.; Lodge, T. P. *Macromolecules* **2002**, *35*, 6997.
(18) Vigild, M. E.; Almdal, K.; Mortensen, K.; Hamley, I. W.; Fairclough, J. P. A.; Ryan, A. J. *Macromolecules* **1998**, *31*, 5702.
(19) Schulz, M. F.; Bates, F. S.; Almdal, K.; Mortensen, K. *Phys. Rev. Lett.* **1994**, *73*, 86.
(20) Schmidt, S. C.; Hillmyer, M. A. *J. Polym. Sci., Part B* **2002**, *40*, 2364.
(21) Sakurai, S.; Umeda, H.; Furukawa, C.; Irie, H.; Nomura, S.; Lee, H. H.; Kim, J. K. *J. Chem. Phys.* **1998**, *108*, 4333.
(22) Hamley, L. W.; Fairclough, J. P. A.; Ryan, A. J.; Mai, S. M.; Booth, C. *Phys. Chem. Chem. Phys.* **1999**, *1*, 2097.
(23) Hajduk, D. A.; Takeuchi, H.; Hillmyer, M. A.; Bates, F. S.; Migild, M. E.; Almdal, K. *Macromolecules* **1997**, *30*, 3788.
(24) Hajduk, D. A.; Ho, R. M.; Hillmyer, M. A.; Bates, F. S.; Almdal, K. *J. Phys. Chem. B* **1998**, *102*, 1356.
(25) Bang, J.; Lodge, T. P.; Wang, X. H.; Brinker, K. L.; Burghardt, W. R. *Phys. Rev. Lett.* **2002**, *89*, 215505.
(26) Sakurai, S.; Umeda, H.; Taie, K.; Nomura, S. *J. Chem. Phys.* **1996**, *105*, 8902.
(27) Jeong, U.; Lee, H. H.; Yang, L. H.; Kim, J. K.; Okamoto, S.; Aida, S.; Sakurai, S. *Macromolecules* **2003**, *36*, 1685.
(28) Ryu, C. Y.; Lodge, T. P. *Macromolecules* **1999**, *32*, 7190.
(29) Kim, J. K.; Lee, H. H.; Ree, M.; Lee, K.-B.; Park, Y. *Macromol. Chem. Phys.* **1998**, *199*, 641.
(30) Sota, N.; Sakamoto, N.; Saijo, K.; Hashimoto, T. *Macromolecules* **2003**, *36*, 4534.
(31) Rancon, Y.; Charvolin, J. *J. Phys. Chem.* **1988**, *92*, 2646.
(32) Clerc, M.; Levelut, A. M.; Sadoc, J. F. *J. Phys. II* **1991**, *1*, 1263.
(33) Fairhurst, C. E.; Holmes, M. C.; Leaver, M. S. *Langmuir* **1997**, *13*, 4964.
(34) Funari, S. S.; Rapp, G. *Proc. Natl. Acad. Sci. U.S.A.* **1999**, *96*, 7756.
(35) Imai, M.; Nakaya, K.; Kato, T. *Phys. Rev. E* **1999**, *60*, 734.
(36) Imai, M.; Saeki, A.; Teramoto, T.; Kawaguchi, A.; Nakaya, K.; Kato, T.; Ito, K. *J. Chem. Phys.* **2001**, *115*, 10525.
(37) Laradji, M.; Shi, A.-C.; Desai, R. C.; Noolandi, J. *Phys. Rev. Lett.* **1997**, *78*, 2577.
(38) Matsen, M. W. *Phys. Rev. Lett.* **1998**, *80*, 4470.
(39) Matsen, M. W. *J. Chem. Phys.* **2001**, *114*, 8165.
(40) Matsen, M. W. *Phys. Rev. Lett.* **1998**, *80*, 201.
(41) Goveas, J. L.; Milner, S. T. *Macromolecules* **1997**, *30*, 2605.
(42) Qi, S.; Wang, Z. G. *Phys. Rev. Lett.* **1996**, *76*, 1679.
(43) Qi, S.; Wang, Z. G. *Phys. Rev. E* **1997**, *55*, 1682.
(44) Qi, S.; Wang, Z. G. *Polymer* **1998**, *39*, 4639.
(45) Nonomura, M.; Ohta, T. *J. Phys.: Condens. Matter* **2001**, *13*, 9089.
(46) Bahiana, M.; Oono, Y. *Phys. Rev. A* **1990**, *41*, 6763.
(47) Nonomura, M.; Yamada, K.; Ohta, T. *J. Phys.: Condens. Matter* **2003**, *15*, L423.
(48) Ohta, T.; Kawasaki, K. *Macromolecules* **1986**, *19*, 2621. Ohta, T.; Kawasaki, K. *Macromolecules* **1990**, *23*, 2413.
(49) Uneyama, T.; Doi, M. *Macromolecules*, submitted.
(50) Teramoto, T.; Nishiura, Y. *J. Phys. Soc. Jpn.* **2002**, *71*, 1611.
(51) Aksimetiev, A.; Fialkowski, M.; Holyst, R. *Adv. Chem. Phys.* **2002**, *121*, 141.
(52) Saeki, A., unpublished results.
(53) Bailey, T. S.; Hardy, C. M.; Epps, T. H., III; Bates, F. S. *Macromolecules* **2002**, *35*, 7007.
(54) Qi, S.; Wang, Z. G. *J. Chem. Phys.* **1999**, *111*, 10681.
(55) Pryamitsin, V. A.; Semenov, A. N.; McLeish, T. C. B. *Eur. Phys. J. E* **2001**, *4*, 161.

MA049687O